Electronic Supplementary Information

One-pot multicomponent synthesis of tetrahydropyridines promoted by luminescent ZnO nanoparticles supported by the aggregates of 6,6-dicyanopentafulvene

Meenal Kataria, Subhamay Pramanik, Manoj Kumar and Vandana Bhalla*

Department of Chemistry, UGC Sponsored Centre for Advanced Studies-1, Guru Nanak Dev University, Amritsar 143005, and Punjab, India

vanmanan@yahoo.co.in

General Experimental Procedures:

Materials and reagents: All reagents were purchased from Aldrich and were used without further purification. THF was dried over sodium and benzophenone as an indicator. UV-vis studies were performed in THF, distilled water and HEPES buffer (0.05 M) (pH = 7.05).

Instrumentation: UV-vis spectra were recorded on a SHIMADZU UV-2450 spectrophotometer, with a quartz cuvette (path length, 1 cm). The cell holder was thermostatted at 25°C. The fluorescence spectra were recorded with a SHIMADZU- 5301 PC spectrofluorimeter. UV-vis spectra were recorded on Shimadzu UV-2450PC spectrophotometer with a quartz cuvette (path length: 1 cm). The cell holder was thermostatted at 25°C. The scanning electron microscope (SEM) images were obtained with a field-emission scanning electron microscope (SEM CARL ZEISS SUPRA 55). The TEM mages was recorded from Transmission Electron Microscope (TEM) - JEOL 2100F. The FT-IR spectra were recorded with VARIAN 660 IR Spectrometer. The dynamic light scattering (DLS) data were recorded with MALVERN Instruments (Nano-ZS). Raman spectrum was recorded with Raneshaw In via reflex micro Raman microscope. The Time resolved fluorescence spectra were recorded with a HORIBA Time Resolved Fluorescence Spectrometer. Polarized optical microscope (POM) images were recorded on NIKON ECLIPSE LV100 POL. Elemental analysis was done using a Flash EA 1112 CHNS/O analyser from Thermo Electron Corporation. ^{1}H and ^{13}C NMR spectra were recorded on a BRUKER-AVANCE-II FT-NMR-AL 500 MHz spectrophotometer using $CDCl_3$, DMSO-d_6 as solvent and tetramethylsilane, $SiMe_4$ as internal standards. Data are reported as follows: chemical shifts in ppm, multiplicity (s = singlet, br = broad signal, d = doublet, t = triplet, m = multiplet), coupling constants *J* (Hz), integration and interpretation. Silica gel 60 (60-120 mesh) was used for column chromatography.

Quantum yield calculations: Fluorescence quantum yield was determined by using optically matching solution of diphenylanthracene (Φ_{fr} = 0.90 in cyclohexane) as standard at an excitation wavelength of 373 nm and quantum yield is calculated using the equation:

$$\Phi_{fs} = \Phi_{fr} \times \frac{1-10^{-ArLr}}{1-10^{-AsLs}} \times \frac{N_s^2}{N_r^2} \times \frac{D_s}{D_r}$$

Φ_{fs} and Φ_{fr} are the radiative quantum yields of sample and the reference respectively, A_s and A_r are the absorbance of the sample and the reference respectively, D_s and D_r are the respective areas of emission for sample and reference. L_s and L_r are the lengths of the absorption cells of sample and reference respectively. N_s and N_r are the refractive indices of the sample and reference solutions (pure solvents were assumed respectively).

UV-vis and fluorescence titrations: The concentration of HEPES buffer (pH = 7.05) is 0.05 M. For each experiment we have taken 3 ml solution which contains solution of derivative **4** in 15 µl (10^{-3}M) of THF solution was diluted with 585 µl of THF and 2.4 ml HEPES buffer (0.05 M, pH = 7.05) or double distilled water. UV-vis and fluorescence titrations were performed with 5.0 µM solutions of ligand in H_2O-THF (8:2, v/v). Typically, aliquots of freshly prepared standard solutions (10^{-1}M to 10^{-3}M) of metal ions such as Zn^{2+}, Hg^{2+}, Cu^{2+}, Fe^{2+}, Fe^{3+}, Co^{2+}, Pb^{2+}, Ni^{2+}, Cd^{2+}, Ag^{+}, Ba^{2+}, Al^{3+}, Mg^{2+}, K^{+} and Na^{+} ions as their perchlorate [$M(ClO_4)_x$; X = 1-3]/chloride [$M(Cl)_x$; X = 1-3] in THF and distilled water were added to record the UV-vis and fluorescence spectra.

Synthesis of ZnO Nanoparticles:

Aqueous solution of 1 M $ZnCl_2$ (550 µL) was added to a 3 ml solution of compound **4** (0.2 mM) in H_2O-THF (8:2, v/v). The reaction was stirred at room temperature for 3h and formations of ZnO nanoparticles take place. A 100 µL solution of the nanoparticles was used as a catalyst in each reaction.

General Procedure for the synthesis of tetrahydropyridine derivatives 12a-f:

To a mixture of β-ketoester **6a/6b** (1.0 mmol / 1 equiv.) and aromatic/aliphatic amine **7a/7b** (2.0 mmol / 2 equiv.), was added 100 µL solution of ZnO nanocatalyst (0.5 mol% / 0.005 equiv.) followed by the addition of aromatic aldehyde (2.0 mmol / 2 equiv.) **8a/8b/8c/8d**. The reaction mixture was stirred at room temperature / 50°C until the completion the reaction as indicated by TLC. A solid separated during the course of the reaction. 5 ml of ethanol was added to this solid which was then filtered, washed and recrystallized from ethanol:$CHCl_3$ (8:2) to give the pure products **12a-f**.

Table S1: Comparison of this method in present manuscript over other procedures for the preparation of ZnO nanoparticles reported in literature.

Sr.no.	Publication	Method of formation of ZnO nanoparticles	Reagent used	Oxidising/ Reducing/ base	Temp. required	Time required	Size of ZnO nanoparticles	Shape of ZnO nanoparticles
1	**Present manuscript**	**Wet Chemical Method**	**Compound 4 in H_2O-THF; 8:2 (v/v)**	**No**	**RT**	**3 h**	**10-20 nm**	**Nanosphers**
2	*Green Chem.*, 2014, **16**, 4922-4930	Sol gel method	Zinc perchlorate, NaOH, Alcohol	Base (NaOH)	500°C	2 h, 6 h	Various sizes	Different Morphologies
3	*J. Mater. Chem. A*, 2014, **2**, 15377-15388	Hydrothermal method	Zinc nitrate hexahydrate, NH_4HCO_3, Hexamethylenetreiamine, methanol	Base (NH_4HCO_3)	RT to ultrasonic to 150°C	24 h	2-50 nm depends upon calcination temperature	Nano sheets
4	*J. Mater. Chem. B*, 2014, **2**, 3956-3964	Hydrolysis method	Zinc acetate, Igepal CO-520, double distilled water	Surfactant (Igepal CO-520)	80°C & 350°C	12 h	50-100 nm diameter of sphere,100-200 nm rod length	Nanosphere & Nanorod
5	*Phys. Chem. Chem. Phys.*, 2014, **16**, 11471-11480	Solvothermal method	Zinc acetate/Zinc chloride, sodium hydroxide, sodium acetate, CTAB	Base (NaOH)	150°C	16 h	Nanosphere (100-150 nm), Nanorods (200-400 nm)	Nanorods & Nanospheres
6	*ACS Appl. Mater. Interfaces*, 2013, **5**, 3026-3032	Solvothermal method	Zinc nitrate hexahydrate, sodium hydroxide, Methanol,Teflon-lined stainless steel autoclave	Base (NaOH)	120°C	24 h	100-150 nm (length)	Nano rods
7	*Chem. Mater.*, 2013, **25**, 1775-1782	Precipitation method	Zinc acetate dehydrate, excess NaOH, Absolute ethanol	Precipitating agent	Ambient temp	30 days	16±3nm, 20±5nm	Nano powder
8	*Chem. Mater.* 2013, **25**, 2927-2933	Electron beam induced method	Zinc nitrate, HMTA, Polyvinylpyrrolidone (PVP)	Surfactant (PVP)	Current density -1 Am^{-2}	36 min	400nm	Wurtizite nanopwder
9	*ACS Sustainable Chem. Eng.*, 2013, **1**, 1207-1213	Electro spinning technique	Zinc nitratehexahydrate, polyvinylpyrrolidon, Ethanol	Capping Agent (polyvinylpyrrolidon)	Calcination at 500°C	1 h	24 nm	Mesoporous nanofibres
10	*Langmuir*, 2012, **28**, 4787-4792	Hydrothermal method	Zinc acetate dihydrate, sodium hydroxide, ethanol, methanol	Base (NaOH)	60°C	2 h	5-10 nm diameter	Nanosphers
11	*Ind. Eng. Chem. Res.*, 2012, **51**, 4922-4926	Hydrothermal method	Zinc chloride, NaOH	Base (NaOH)	200°C	24 h	10-20µm, 50-100nm	Bullet shaped (10-20 µm), rod shaped (50-100nm)
12	*Chem. Mater.*, 2011, **23**, 5237-	i) Metal organic precursor (MZI)	i) Dimethyl Zinc, toluene, Diethyl	Oxidizing agent (O_2)	-78°C, 120°C	Several days	3-50 nm diameter	Nano spheres

	5242	ii) Evaporation & thermal decomposition	ether, isopropanol, -78˚c ii) O_2 , 85 to 120˚C					
13	*Crystal Growth & Design*, 2010, **10**,1500-1507	Hydrothermal synthesis	Zinc nitrate , hexamethylenetetramine ($C_6H_{12}N_4$) and PEG, ITO	Base ($C_6H_{12}N_4$)	95°C	4 h	Spheres with diameter (100 nm)	Nano spheres and Nano rods
14	*Chem.Mater*., 2010, **22**, 218-225	Chemical vapour synthesis	Diethyl Zinc,O_2, He gas	Oxidizing agent (O_2)	800-900°C	-	11.7-18.3 nm	Nano crystals

Table S2: Comparison of catalytic activity ZnO nanoparticles for Synthesis of tetrahydropyridine derivatives over other catalytic systems reported in literature.

Sr. No.	Publication	Catalyst used	Use of noble metal	Reagent used other than reactant and catalysts	Catalyst Amount (mol%)	Solvent	Nano catalysis	Re use	Reaction time	Temp (in ˚C)	Purification	Isolated Yield (%)
1.	**Present manuscript**	**ZnO NPs**	**No**	**No**	**0.5 mol%**	**Nearly Solvent Free**	**Yes**	**Yes**	**3 h / 9 h**	**RT / 50°C**	**Separated by filtration**	**91%**
2.	*Org. Lett.*, 2014, **16**, 4520-4523	$LiBr.H_2O$	No	No	30 mol%	Nitro Methane (explosive)	No	Yes	Up to 11h	100°C	Preparative TLC	62-99%
3.	*Ultason. Sonochem.*, 2014, **21,**1150-1154	ZrP_2O_7	Yes	No	5 mol%	Methanol	Yes	Yes	60-75 min	Ultra sond	-	89%
4.	*Chem. Commun.*, 2013,**49**, 3543-3545	Phosphine and amine catalyst	No	No	20 mol%	THF	No	-	24h	66°C	-	49-79%-
5.	*Org. Biomol. Chem.*, 2014, **12**, 2394-2403	$Pd(OAc)_2$	Yes	K_2CO_3, BINAP, argon atmosphere	10 mol%	Dioxane (carcinogen nic)	No	No	50 min	120°C	Column chromatography	98%
6.	*J. Org. Chem.* 2013, **78**, 5751-5755	$Sc(OTf)_3$	No	1,10 - phenanthroline	10 mol%	DCM	No	No	24-48 h	Reflux	Column chromatography	51-66%
7.	*Org. Lett.*, 2012, **14**,5290-5293	Organocatayst and Au catalyst	Yes	Bronsted acid	5 mol%	Toluene (toxic)	No	No	3-24 h	RT to 100	Flash chromatography	Up to 72%
8.	*J. Org. Chem.*, 2012, **77**, 4252-4260	DABCO	No	No	-	EtOH	No	No	5-8 h	Reflux	-	73-88%
9.	*ACS Comb. Sci.*, 2011, **13**, 181-185	Ceric ammonium nitrate	No	No	15 mol%	ACN (carcinogen nic)	No	No	22 h	RT	Column chromatography	85%
10.	*J. Am. Chem. Soc.*, 2009, **131**, 6318-6319	PPh_3	No	No	-	CH_2Cl_2 (flammable)	No	No	72 h	RT	Flash chromatography	37-88%
11.	*Angew. Chem. Int. Ed.*, 2008, **47**, 4851-4854	$Pd(PPh_3)_2$	Yes	K_2CO_3, HCHO	2 mol%	THF(flammable, skin dehydration)	No	No	1-8 h	50°C	-	7-88%
12.	*Acc. Chem. Res.*, 2000, **22**, 225-233	$IrH(CO)(PPh_3)_3$	Yes	No	3 mol%	THF	No	Yes	-	120°C	-	96%

Synthetic scheme of compound 4:

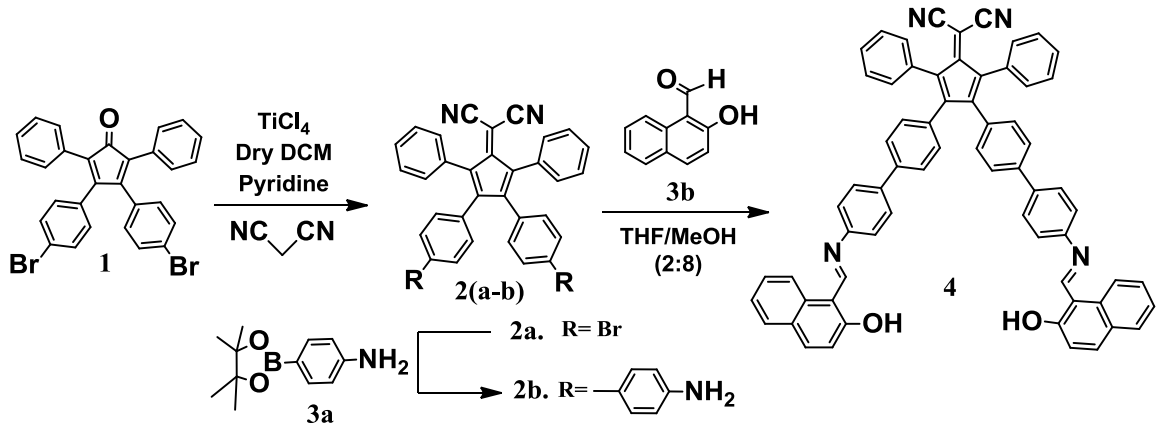

Scheme 1: Synthesis of 6, 6- dicyanopentafulvene derivatives **4**

Synthesis of compound 2a: To a solution of **1**, 3,4-bis(4-bromophenyl)-2,5-diphenylcyclopenta-2,4-dienon (0.50 g, 0.92 mmol) and malononitrile (0.31 g, 4.61 mmol) in 20 ml dry CH_2Cl_2 were added 0.75 ml pyridine and 0.50 ml of $TiCl_4$ under N_2 atmosphere. The reaction mixture was refluxed overnight at 80°C. After that the reaction mixture was allowed to cool to room temperature. The mixture was then diluted with dichloromethane and extracted with 2 N HCl solutions in water. The organic layer was separated and dried over anhydrous Na_2SO_4. The solvent was evaporated under reduced pressure to get the crude product. The organic layer was evaporated, and the compound was purified by column chromatography using (40:60) ($CHCl_3$:Hexane) as an eluent to give 0.28 g (yield 52%) of compound **2a** as a green solid; mp: >280°C (Scheme 1). The structure of compound **2a** was confirmed from its spectroscopic and analytical data. ^{1}H NMR (500 MHz, $CDCl_3$, ppm) δ = 7.45-7.41 (m, 6H, ArH), 7.31-7.28 (m, 4H, ArH), 7.25 (d, *J* = 10Hz, 4H, ArH), 6.74 (d, *J* = 10Hz, 4H, ArH). ^{13}C NMR (125 MHz, $CDCl_3$, ppm) δ = 167.64, 149.32, 132.34, 131.25, 131.19, 131.06, 130.99, 130.91, 129.41, 128.94, 123.41, 111.08, 87.40. ESI-MS mass spectrum of compound **2a** showed a parent ion peak, m/z = 590.4344 $[M+H]^+$. The FT-IR spectrum of compound **2a** showed stretching band 2220 cm^{-1} corresponds to -CN group. Elemental analysis: Calculated for $C_{32}H_{18}Br_2N_2$: C 65.11; H 3.07; N 4.75; Found: C 65.10%; H 3.08%; N 4.77%.

Synthesis of compound 2b: To a solution of **2a** (0.3g, 0.5082 mmol) and **3a** (0.289 g, 1.32 mmol) in 20 ml 1,4-dioxane were added K_2CO_3(0.56 g, 4.06 mmol), distilled H_2O (2.10 ml) followed by [$Pd(PPh_3)_4$] catalyst (0.213 g, 0.304mmol) under N_2 atm., then the reaction

mixture was refluxed overnight. 1,4-Dioxane was then distilled off under vacuum and the residue so obtained was treated with water, extracted with $CHCl_3$, and dried over anhydrous Na_2SO_4. The organic layer was evaporated, and the compound was purified by column chromatography using 80:20 ($CHCl_3$:hexane) followed by recrystallized with 5:1 ($CHCl_3$:MeOH) to give 0.174g (56%) of compound **2b** as orange brown solid; mp: >280°C (Scheme 1). The structure of compound **2b** was confirmed from its spectroscopic and analytical data. ^{1}H NMR (500 MHz, $CDCl_3$, ppm) δ = 7.71-7.67 (m, 8H, ArH), 7.57 (t, *J* = 7.5 Hz, 6H, ArH), 7.50 (d, *J* = 5 Hz, 4H, ArH), 7.48 (d, *J* = 5 Hz, 4H, ArH), 7.47 (d, *J* = 5 Hz, 2H, ArH), 6.72 (t, *J* = 5 Hz, 2H, ArH), 3.75 (s, 4H, -NH). ^{13}C NMR (125 MHz, $CDCl_3$, ppm) δ = 170.42, 150.72, 144.91, 143.04, 138.39, 135.88, 132.90, 132.14, 132.06, 131.96, 131.92, 128.56, 128.46, 127.84, 113.90, 87.58. ESI-MS mass spectrum of compound **2a** showed a parent ion peak, m/z = 637.4234 $[M+Na]^+$. The FT-IR spectrum of compound **2a** showed stretching band 2224 and 3366 cm^{-1} corresponds to -CN and -NH_2 group. Elemental analysis: Calculated for $C_{44}H_{30}N_4$: C 85.97; H 4.92; N 9.11; Found: C 85.96%; H 4.91%; N 9.09%.

Synthesis of compound 4: A clear solution of compound **2b** and **3b,** β-hydroxy naphthaldehyde in dry THF:MeOH (4:6) was stirred at 80°C. After 24 h, the reaction mixture turned turbid. The reaction mixture was concentrated under the reduced pressure and dry methanol was poured into it, solid appears. The solid was filtered and recrystallized from methanol to afford the light yellow coloured compound **4** (0.064g, 85%); mp: >280°C (Scheme 1). The structure of compound **4** was confirmed from its spectroscopic and analytical data. ^{1}H NMR (500 MHz, DMSO-d_6, ppm) δ = 15.88 (s, 2H, -OH), 9.73 (s, 2H, -HC=N), 8.54 (d, *J* = 10Hz , 2H, ArH), 8.15 (d, *J* = 5 Hz, 2H, ArH), 7.95 (d, *J* = 10Hz, 4H, ArH), 7.90 (d, *J* = 10Hz, 4H, ArH), 7.79 (t, *J* = 7.5 Hz, 8H, ArH), 7.57 (q, *J* = 10Hz, 6H, ArH), 7.37 (t, *J* = 7.5 Hz, 6H, ArH), 7.25 (d, *J* = 10 Hz, 4H, ArH), 7.01 (t, *J* = 7.5 Hz, 2H, ArH). ^{13}C NMR (125 MHz, $CDCl_3$, ppm) δ =171.14, 167.77, 155.42, 149.37, 138.03, 132.33, 131.34, 131.21, 131.09, 130.98, 130.94, 129.44, 128.97, 123.43, 119.46, 114.23, 111.08, 87.30. ESI-MS mass spectrum of compound **4** showed a parent ion peak, m/z = 923.3618 $[M+H]^+$. The FT-IR spectrum of compound **4** showed stretching bands at 1621 and 2225 cm^{-1} corresponds to -HC=N and -CN group. Elemental analysis: Calculated for $C_{70}H_{48}N_6$: C 85.88; H 4.59; N 6.07; Found: C 85.86%; H 4.58%; N 6.07%.

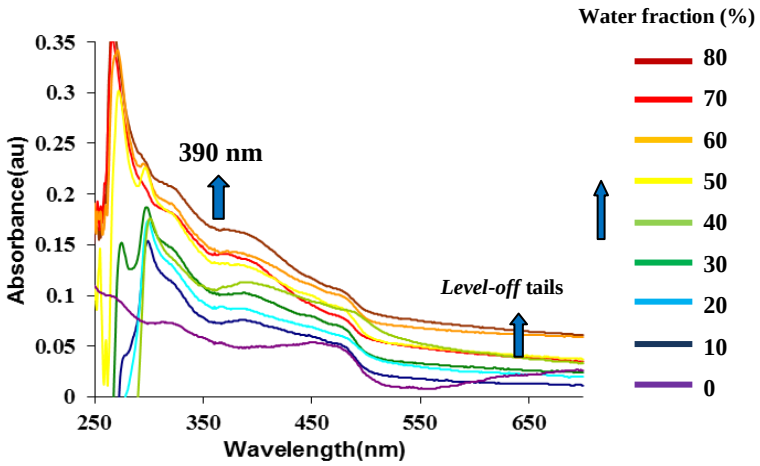

Fig. S1A: UV-vis spectra showing the change in absorbance of compound **4** (5 µM) in various H_2O-THF mixture (0 to 80% volume fraction of water in THF).

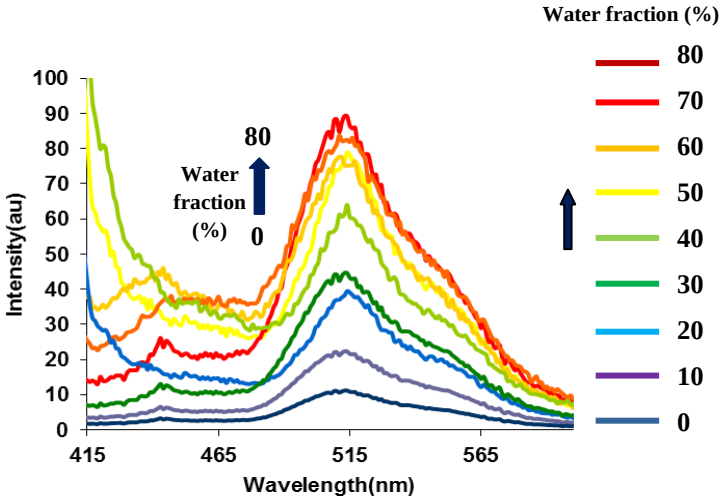

Fig. S1B: Fluorescence spectra of compound **4** (5 µM) showing the variation of fluorescence intensity in H_2O-THF mixture (0 to 80% volume fraction of water in THF); λ_{ex}= 390 nm.

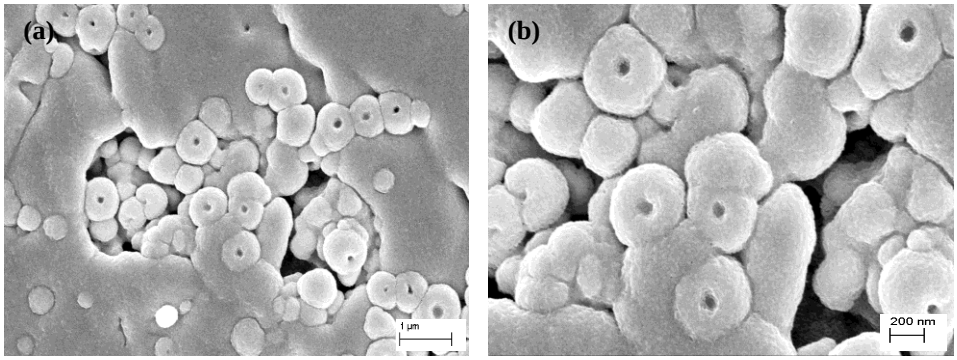

Fig. S2A: Photographs of SEM images of pot shaped aggregates of derivative **4** in H_2O-THF (8:2, v/v) mixture.

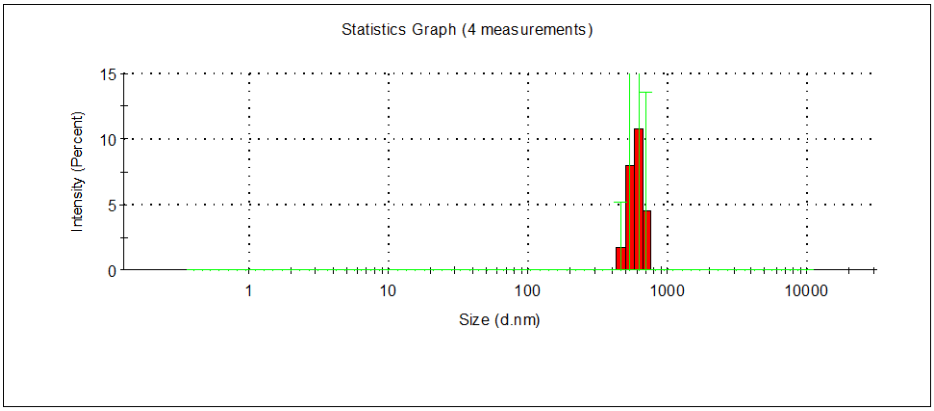

Fig. S2B: Dynamic light scattering (DLS) results showing the particle size diameter of aggregates of **4** in H_2O-THF (8:2, v/v) mixture.

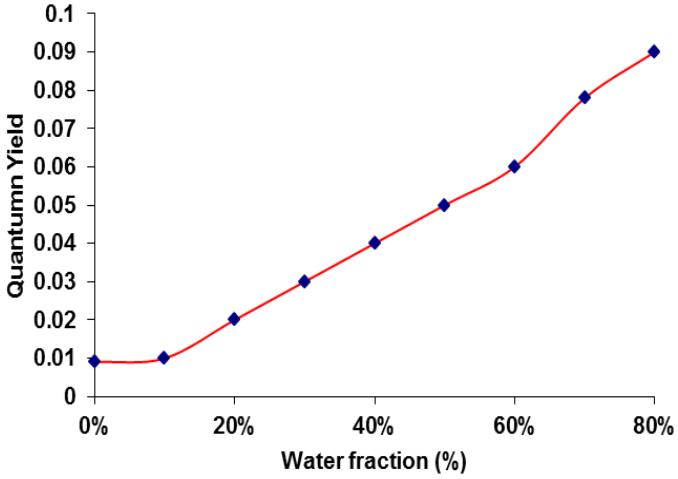

Fig. S3A: Variation in quantum yield value with the variation of water fractions (0 to 80% volume fraction of water in THF); λ_{ex} = 390 nm.

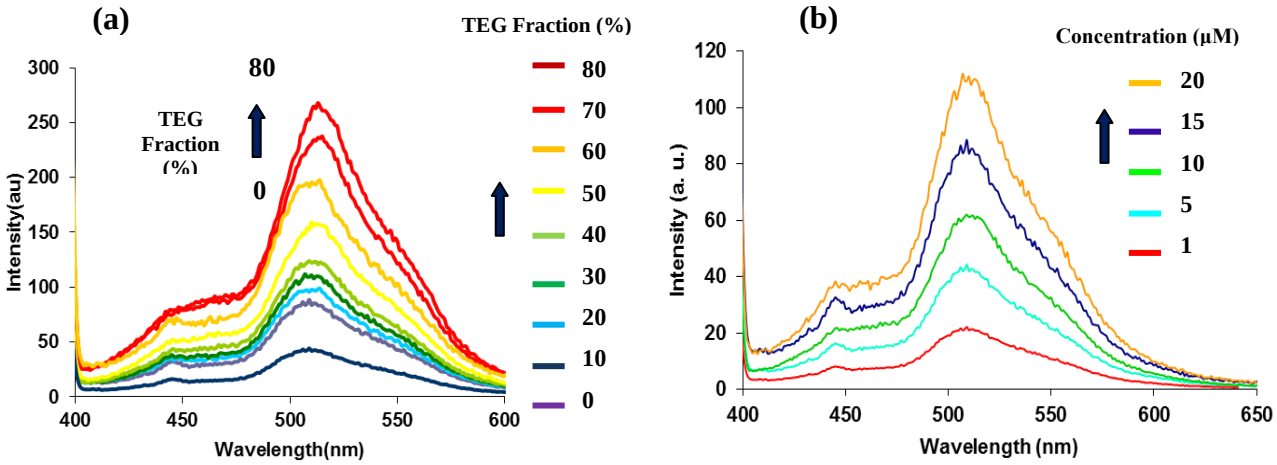

Fig. S3B: (a) Fluorescence spectra of compound **4** (5 μM) showing the variation of fluorescence intensity in TEG-THF mixture (0 to 80% volume fraction of TEG in THF), λ_{ex} = 390 nm; (b) Fluorescence spectra of compound **4** showing the variation of fluorescence intensity with different concentration of **4** (1μM - 20μM) in THF; λ_{ex} = 390 nm.

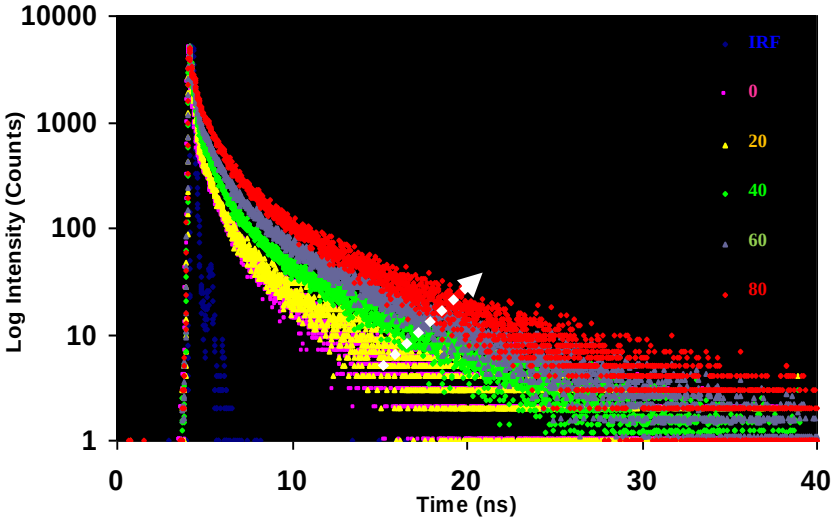

Fig. S4: Exponential fluorescence decays of **4** on addition of water fraction measured at 510 nm. Spectra were acquired in Water-THF mixture (0 to 80% volume fraction of water in THF), λ_{ex}= 377 nm.

Water Fraction	**Quantumn Yield**	**A_1/A_2**	**τ_1 (ns)**	**τ_2 (ns)**	**τ_{avg} (Average lifetime, ns)**	**k_f (10^9 S^{-1})**	**k_{nr} (10^9 S^{-1})**
0%	0.009	82/18	0.5	1.73	0.78	0.01154	1.27
80%	0.09	56/44	0.74	3.5	2.5	0.032	0.368

Table S3: Fluorescence lifetime of derivative **4** in absence and presence of water (80%) in THF at 510 nm. **A_1**, **A_2:** fractional amount of molecules in each environment. **τ_1**, **τ_2** and **τ_{avg}:** bi-exponential and average life time of aggregates in 80 vol% of water in THF; **k_f:** radiative rate constant ($k_f = \Phi_f/\tau_{avg}$); **k_{nr}:** non-radiative rate constant [$k_{nr} = (1- \Phi_f)/\tau_{avg}$]; λ_{ex}= 377 nm.

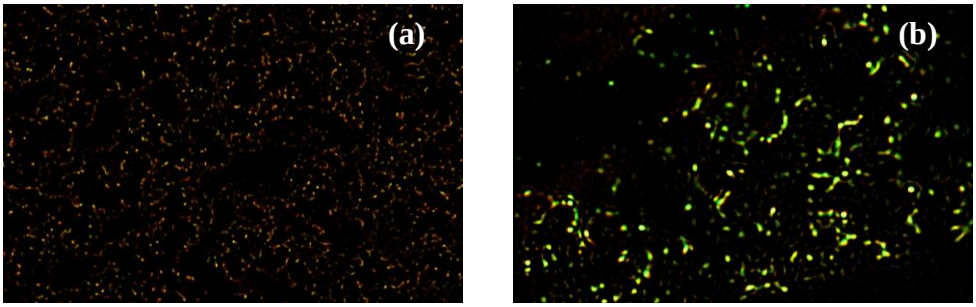

Fig. S5A: Polarized optical microscopic images of (a) derivative **4** and (b) in the presence of Zn^{2+} ions at room temperature through crossed polarizing filters.

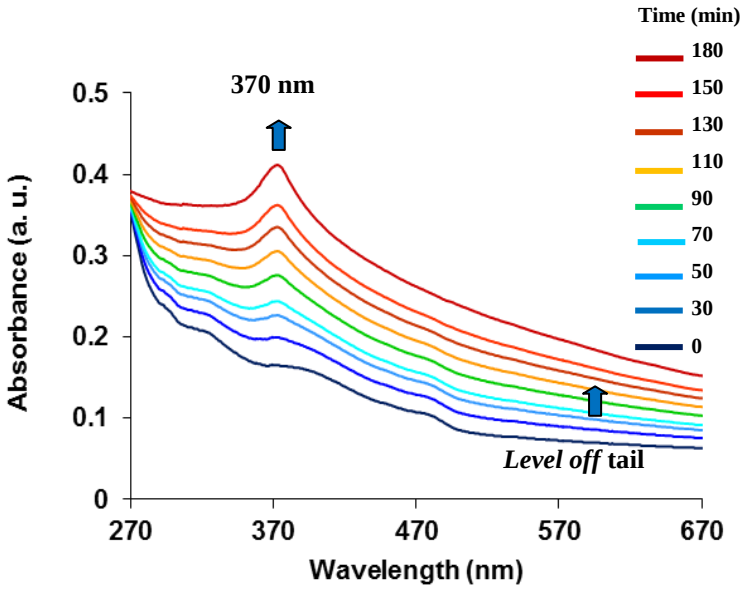

Fig. 5B: UV-vis spectra of aggregates of compound **4** (5 µM) in presence of Zn^{2+} ions (0-350 equiv.) in H_2O-THF (8:2, v/v) mixture within 180 min.

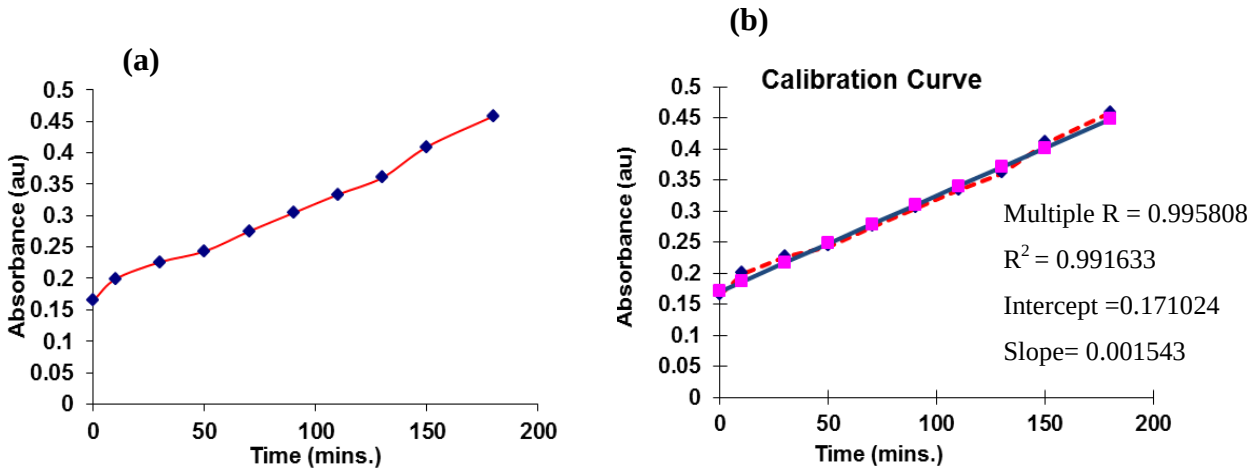

Fig. S6: Graphical representation of the rate of formation of ZnO nanoparticles of derivative **4**. (a) Time (mins.) vs. absorbance plot at 370 nm (b) regression plot of a.

The first order rate constant for the formation of ZnO nanoparticles was calculated from the changes of intensity of absorbance of aggregates of derivative **4** in the presence of Zn^{2+} ions at different time interval.

From the time vs. absorbance plot at fixed wavelength 370 nm by using first order rate equation, we get the rate constant = k = slope×2.303= **5.9×10^{-5} sec^{-1}.**

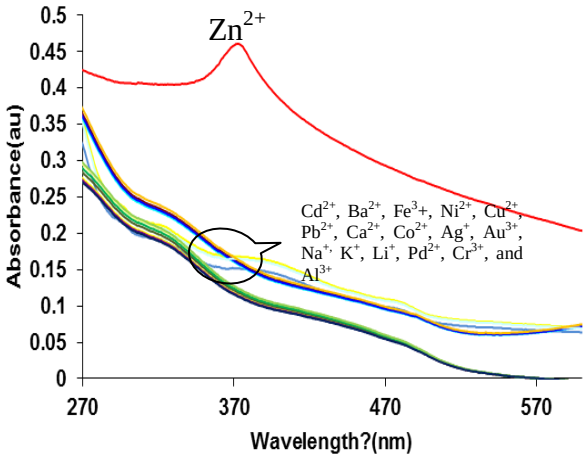

Fig. S7A: UV-vis spectra of derivative **4** (5 µM) upon additions of 350 equiv. of various metal ions as their **chloride salt** in H_2O-THF (8:2, v/v) mixture after 3 h.

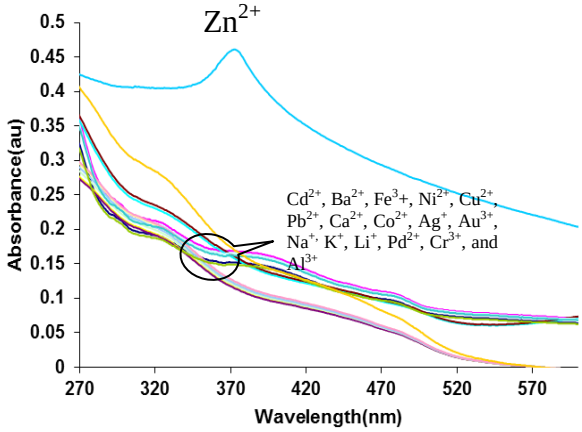

Fig. S7B. : UV-vis spectra of derivative **4** (5 µM) upon additions of 350 equiv. of various metal ions as their **perchlorate salts** in in H_2O-THF (8:2, v/v) mixture after 3 h.

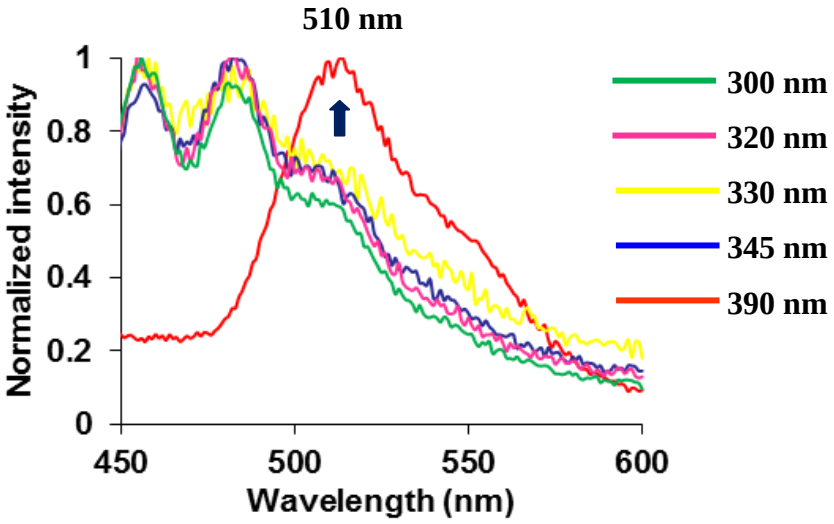

Fig. S8A: Normalized emission spectra of ZnO nanoparticles after the addition of Zn^{2+} ions in the aggregates of **4** in H_2O-THF (8:2) mixture buffered with HEPES; pH = 7.05 at different excitation wavelengths (300, 320, 330, 345, 390 nm).

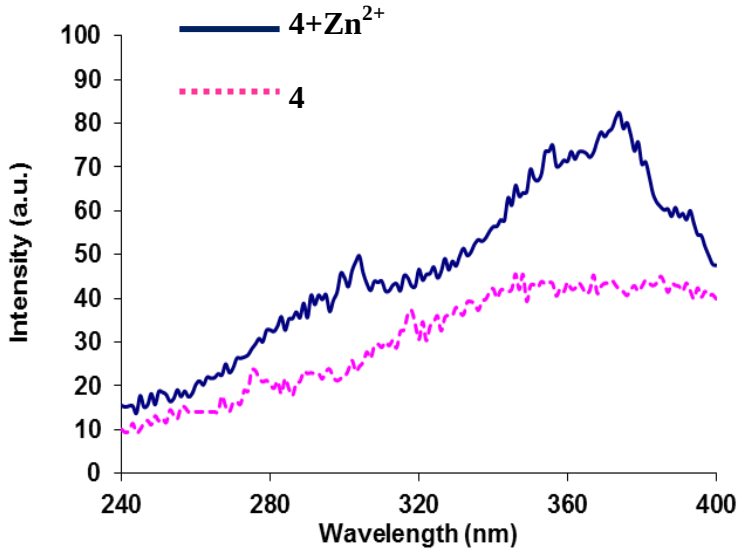

Fig. S8B: Showing the excitation spectra of **4** in H_2O-THF (8:2) mixture buffered with HEPES; pH = 7.05; before and after the addition of Zn^{2+} ions for the emission at 510 nm.

Multiple R = 0.967974

R^2 = 0.936975

Standard deviation = 0.008

Observation = 13

Slope = 25216.97

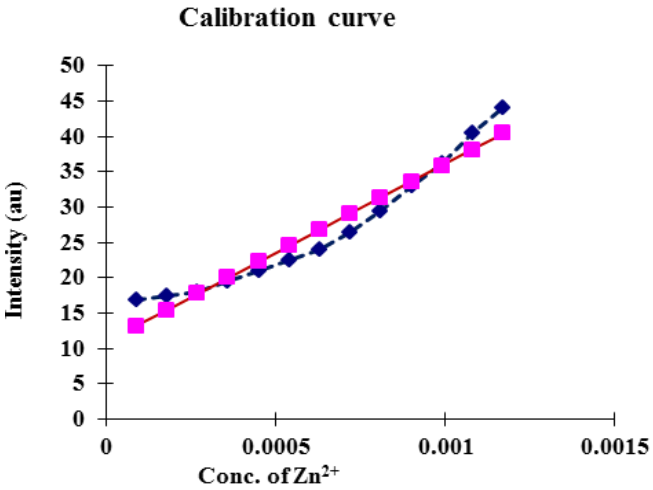

Fig. S9: Calibrated curve showing the Fluorescence intensity of compound **4** at 510 nm as a function of Zn^{2+} ions concentration (equiv.) in H_2O-THF (8:2, v/v); λ_{ex}= 390.

The detection limit was calculated based on the fluorescence titration. To determine the S/N ratio, the emission intensity of receptor **4** without Zn^{2+} was measured by 10 times and the standard deviation of blank measurements was determined.

The detection limit is then calculated with the following equation:

DL = 3 × SD/S

Where SD is the standard deviation of the blank solution measured by 10 times; S is the slope of the calibration curve.

From the graph we get slope

S = 25216.97, and SD value is 0.008

Thus using the formula we get the Detection Limit

(DL) = 3 × 0.008/25216.97 = 950×10^{-9} M = 95×10^{-8} M

i.e., probe **4** can detect Zn^{2+} ions in this minimum concentration through fluorescence method.

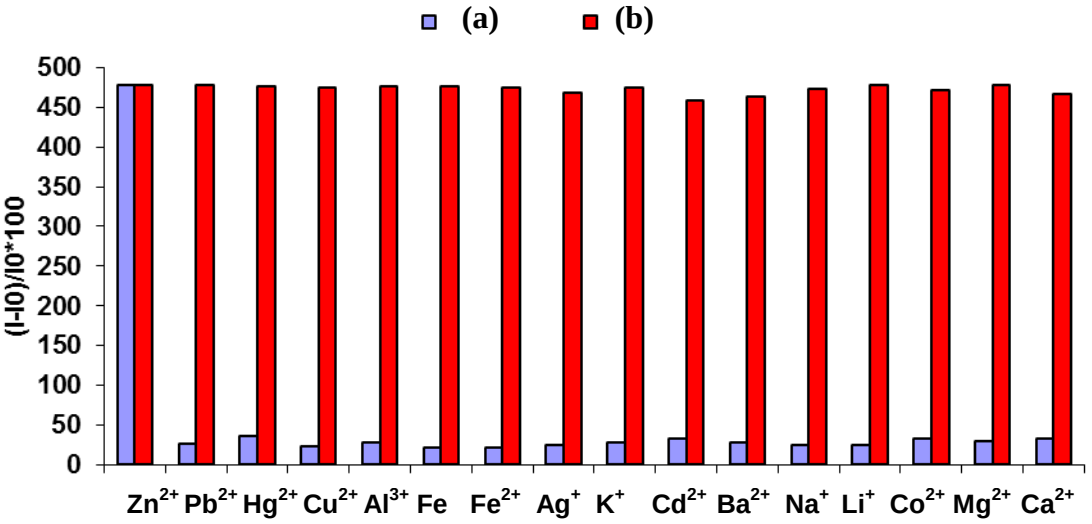

Fig. S10A: Fluorescence response of derivative **4** (5 μM) to various metal ions of **chloride** salts in H_2O-THF (8:2) mixture buffered with HEPES; pH = 7.05; λ_{ex} = 390 nm. Bars represent the emission intensity ratio $(I–I_0)/I_0 \times 100$ (I_0 and I are the initial and final fluorescence intensity at 510 nm after the addition of various metal ions); (a) The sky blue bars represent the addition of individual metal ions, (b) the red bars represent the change in the emission that occurs upon the subsequent addition of Zn^{2+} (350 equiv.) to the above solution.

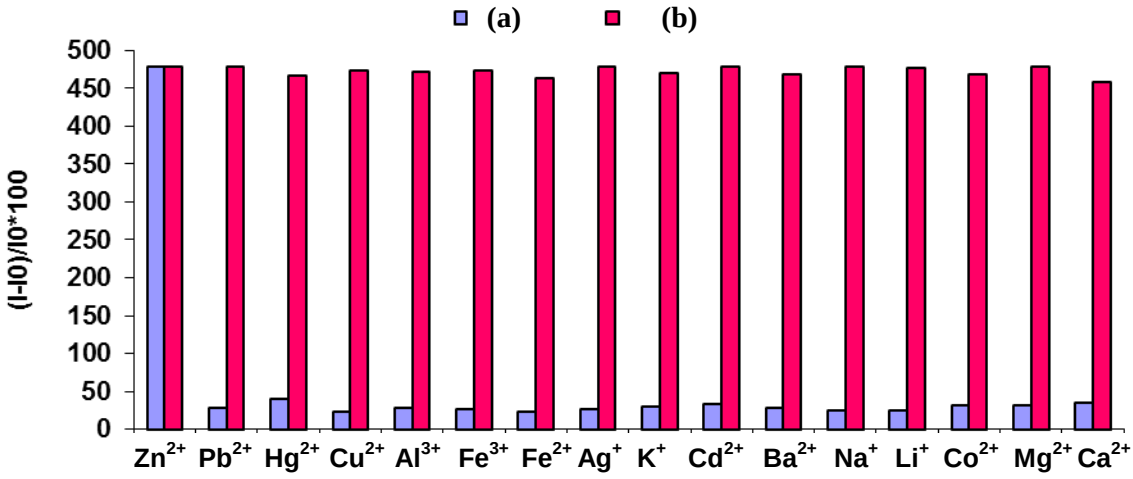

Fig. S10B: Fluorescence response of derivative **4** (5 μM) to various metal ions of **perchlorate** salts in H_2O-THF (8:2) mixture buffered with HEPES; pH = 7.05; λ_{ex} = 390 nm. Bars represent the emission intensity ratio $(I–I_0)/I_0 \times 100$ (I_0 and I are the initial and final fluorescence intensity at 510 nm after the addition of various metal ions); (a) The sky blue bars represent the addition of individual metal ions, (b) the red bars represent the change in the emission that occurs upon the subsequent addition of Zn^{2+} (350 equiv.) to the above solution.

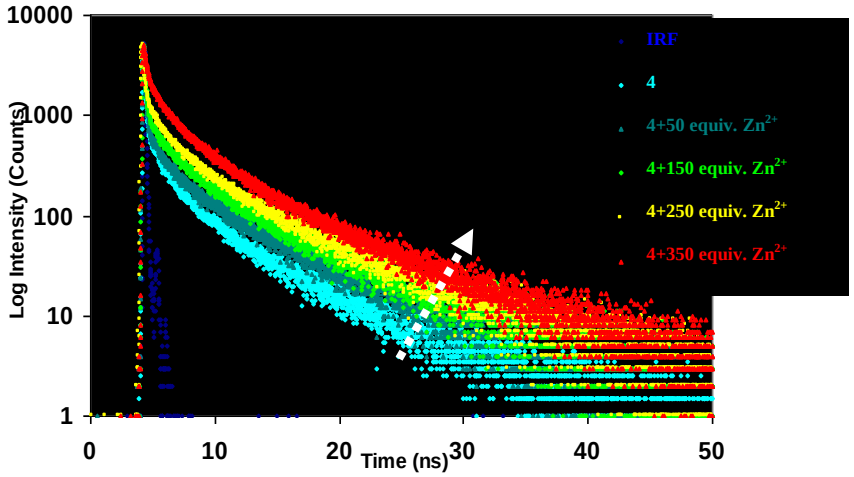

Fig. S11: Exponential fluorescence decays of **4** on addition of different amount of Zn^{2+} ions within 180 minutes measured at 510 nm. Spectra were acquired in H_2O-THF (8:2, v/v) mixture buffered with HEPES; pH = 7.05, λ_{ex}= 377 nm.

Zn^{2+} (equiv.)	Quantumn Yield	A_1/A_2	τ_1 (ns)	τ_2 (ns)	τ_{avg} (Average lifetime, ns)	k_f (10^9 S^{-1})	k_{nr} (10^9 S^{-1})
0	0.009	56/44	0.74	3.5	2.5	0.032	0.368
350	0.36	5/95	1.78	9.6	6.7	0.053	0.095

Table S4: Fluorescence lifetime of derivative **4** in absence and presence of Zn^{2+} ions (350 equiv.; 180 minutes) in H_2O-THF (8:2, v/v) mixture buffered with HEPES; pH = 7.05; at 510 nm. **A_1, A_2:** fractional amount of molecules in each environment. **τ_1, τ_2** and **τ_{avg}:** bi-exponential and average life time of aggregates in 80 vol% of water in THF; **k_f:** radiative rate constant (k_f = Φ_f/τ_{avg}); **k_{nr}:** non-radiative rate constant (k_{nr} = (1- Φ_f)/τ_{avg}); λ_{ex}= 377 nm.

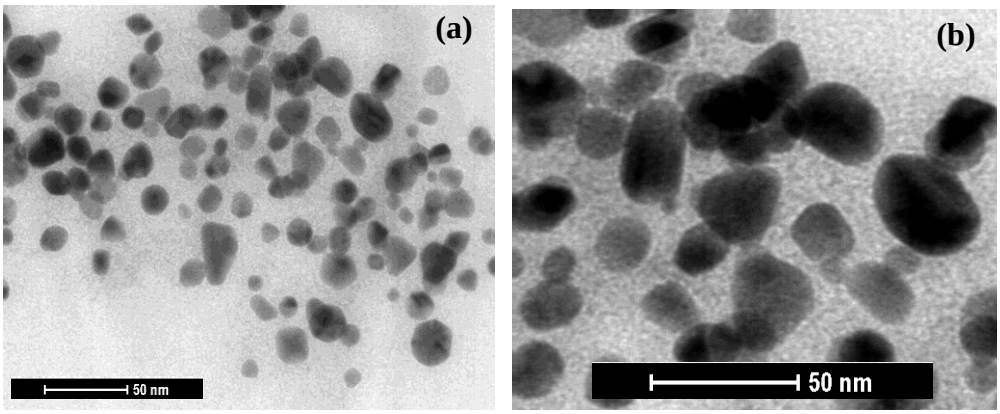

Fig. S12A: TEM images (a-b) of ZnO nanoparticles.

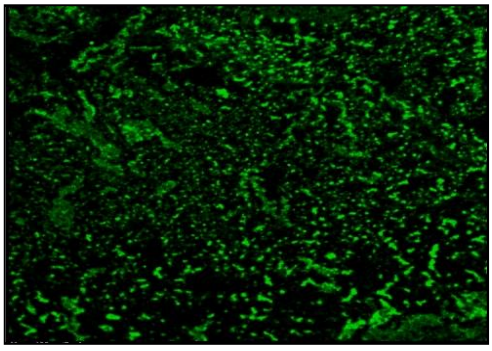

Fig. S12B: Confocal Images of ZnO nanoparticles in a solvent mixture of H_2O-THF (8:2, v/v). λ_{ex} = 405 nm.

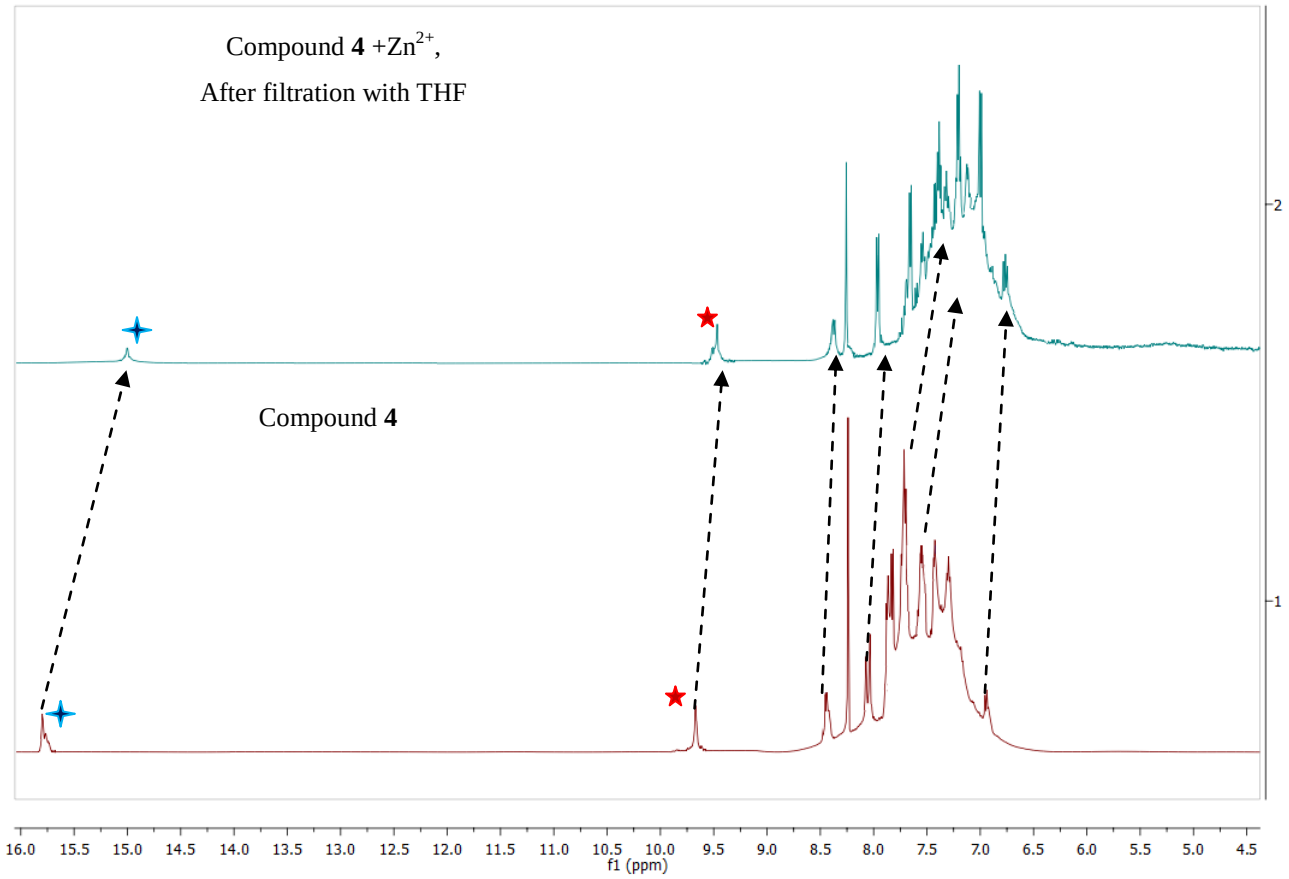

Fig. S13: Overlay ^{1}H NMR spectra of derivative **4** in DMSO-d_6 and ZnO nanoparticles of derivative **4** after filtration with THF.

Compound 4 (δ_4, ppm)	**Compound 4 + Zn^{2+}**, After filtration by THF (δ_F, ppm)	$\Delta\delta_1 = \delta_4 - \delta_F$
15.88 (-OH)	15.10	0.78
9.73 (-N=CH)	9.42	0.31
8.54 (d, aromatic)	8.35	0.19
8.15 (d, aromatic)	7.92	0.23
7.95 (d, aromatic)	7.70	0.25
7.79 (t, aromatic)	7.44	0.35
7.57 (q, aromatic)	7.20	0.37
7.37 (t, aromatic)	7.07	0.30
7.01 (t, aromatic)	6.77	0.24

Table S5: Change in chemical shift (δ) value of ^{1}H NMR spectra of derivative **4** in DMSO-d_6 and ZnO nanoparticles of derivative **4** after filtration with THF.

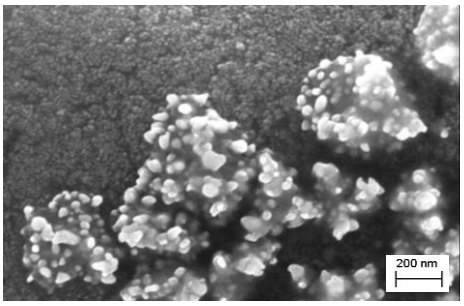

Fig. S14A: Photographs of SEM images showing aggregates of **4** in H_2O-THF (8:2, v/v) after treatment of $ZnCl_2$ with aggregates of derivative **4**.

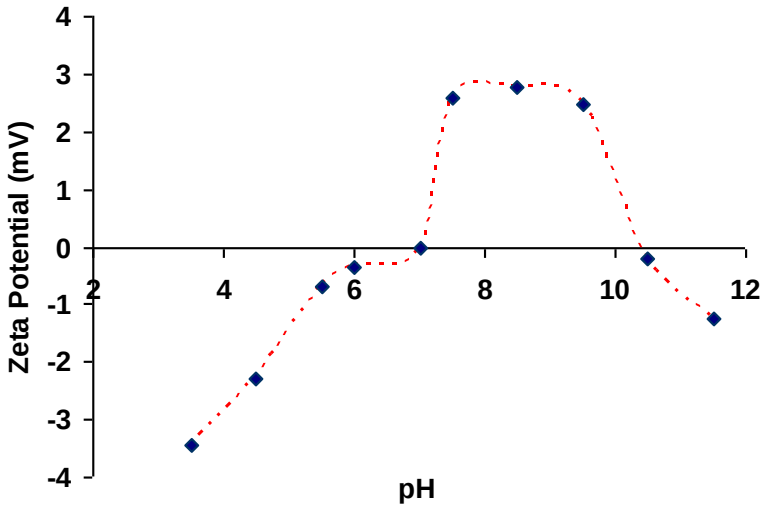

Fig. S14B: Variation of Zeta Potential of ZnO nanoparticles at various pH after the addition of Zn^{2+} ion to the solution of derivative **4** in H_2O-THF (8:2, v/v).

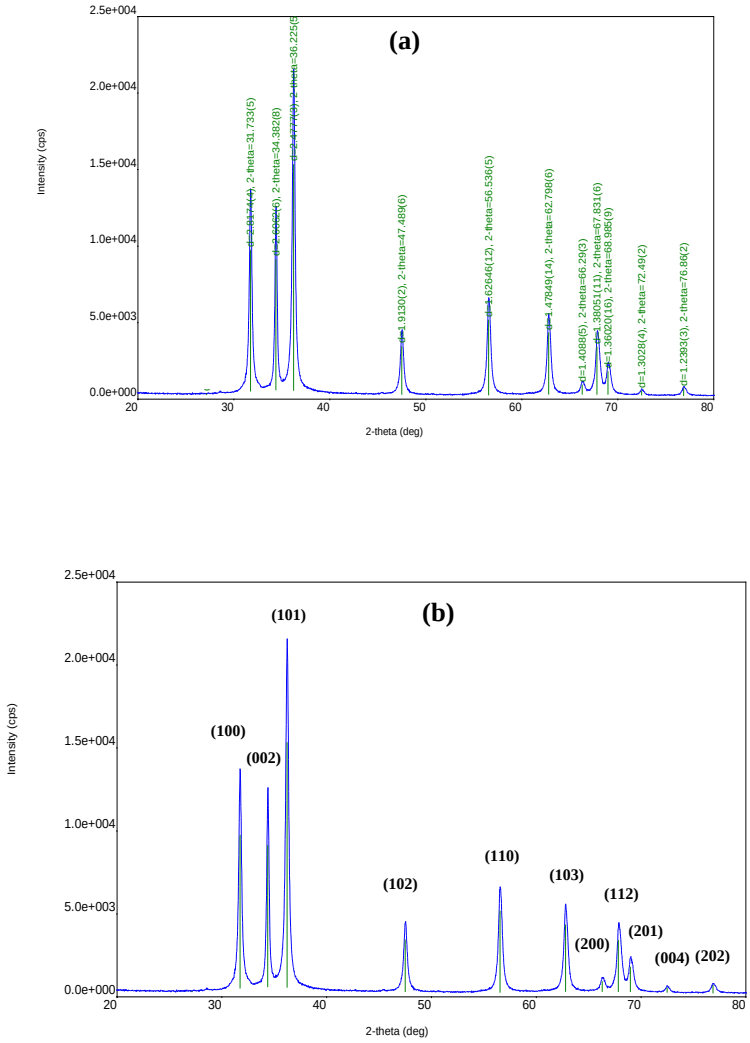

Fig. S15: Representative XRD diffraction patterns of ZnO nanoparticles prepared by derivative **4**.

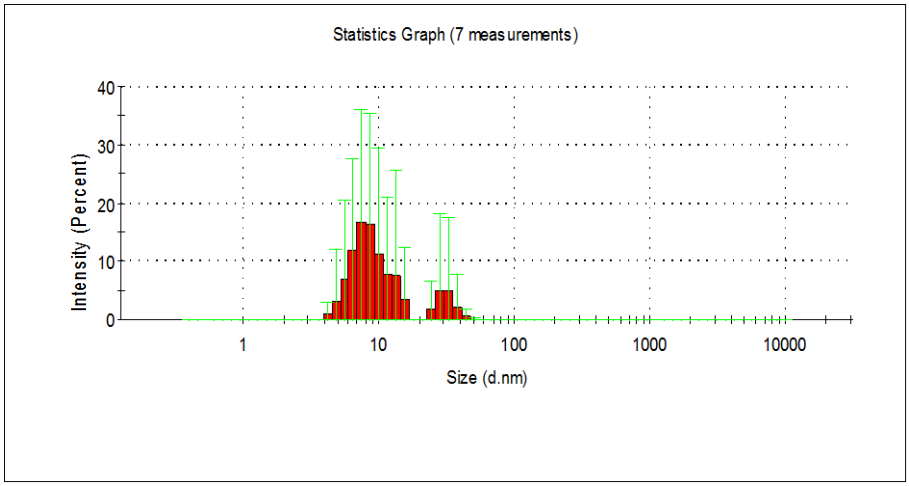

Fig. S16A: Dynamic light scattering (DLS) results showing the particle size diameter of ZnO nanoparticles prepared by aggregates of **4**.

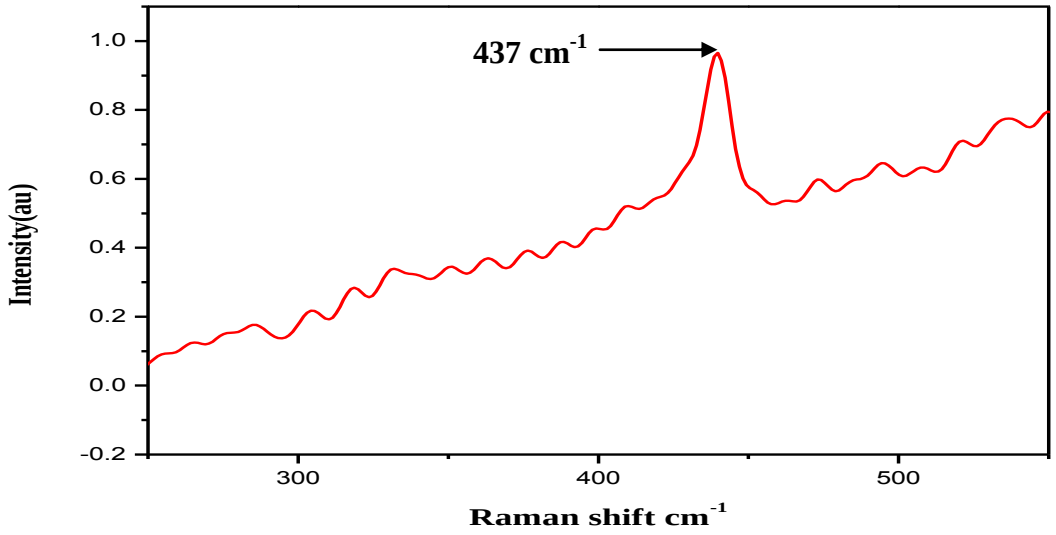

Fig. S16B: Raman spectrum showing 437 cm^{-1} indicates the formation of spherical ZnO nanoparticles prepared by aggregates of **4**.

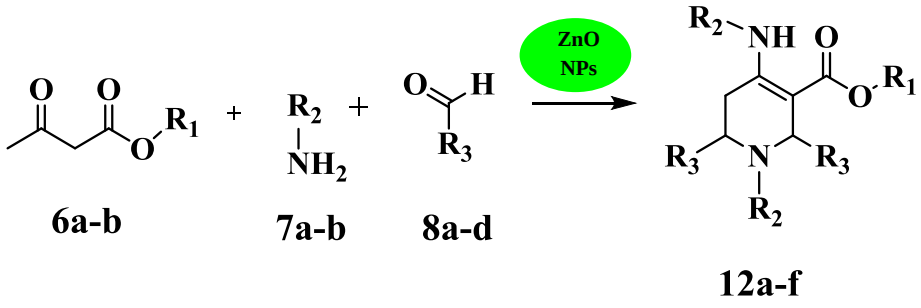

Scheme 2: Catalytic applications: one pot Multicomponent Synthesis of Tetrahydropyridines **12a-f**.

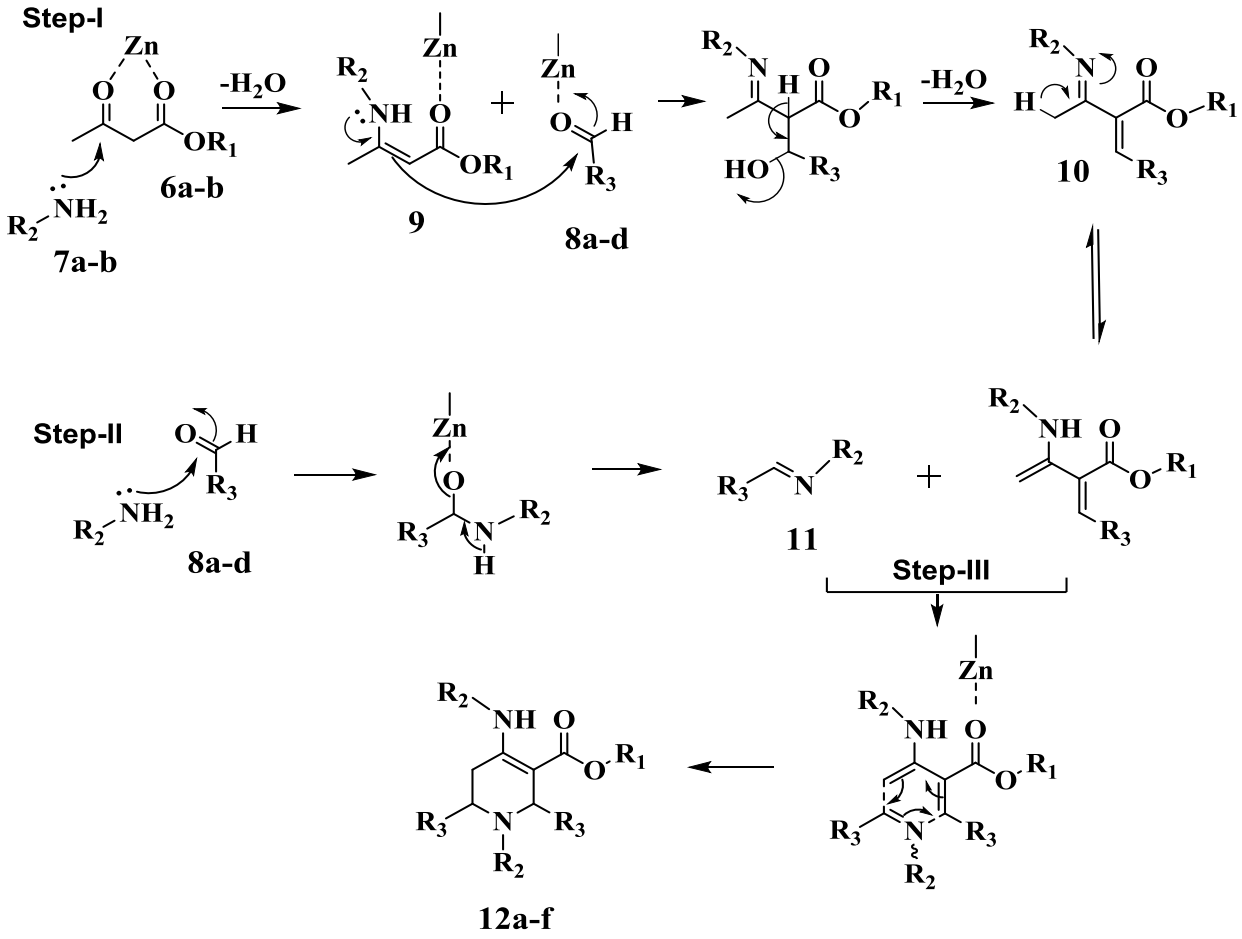

Scheme 3: Proposed mechanism of one pot Multicomponent Synthesis of tetrahydropyridines **12a-f** in presence of ZnO nanoparticles.

Table S6: ZnO nanoparticles catalysed one pot multicomponent reactions of aromatic/primary amine with aromatic aldehyde and β-ketoester for the synthesis of tetrahydropyridines **12a-f**.

Reactants			Products	Temp.	Time	Yield	Melting Point
6a-b	**7a-b**	**8a-d**	**12a-f**				
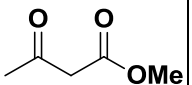 **6a**	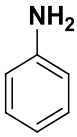 **7a**	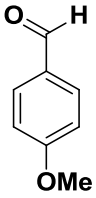 **8a**	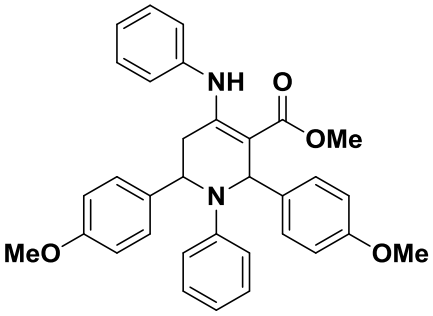 **(12a)**	RT	2.5 h	91%	189-190ºC
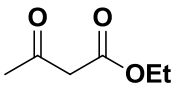 **6b**	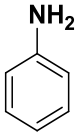 **7a**	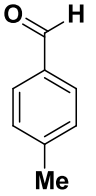 **8b**	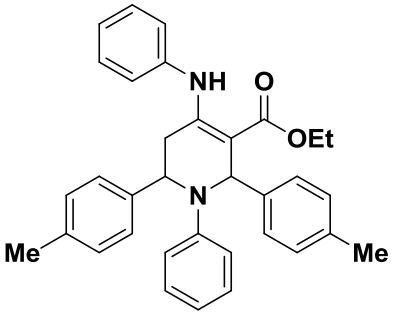 **(12b)**	RT	3h	89%	229-230ºC
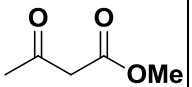 **6a**	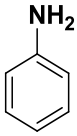 **7a**	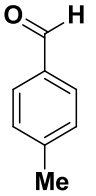 **8b**	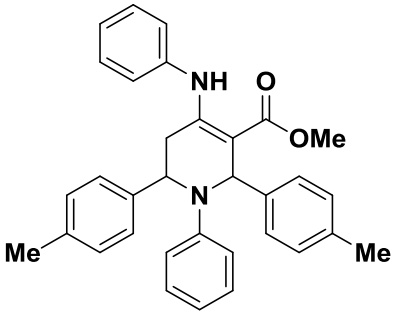 **(12c)**	RT	3h	89%	212-213ºC
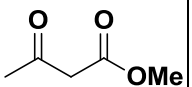 **6a**	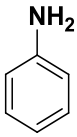 **7a**	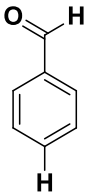 **8c**	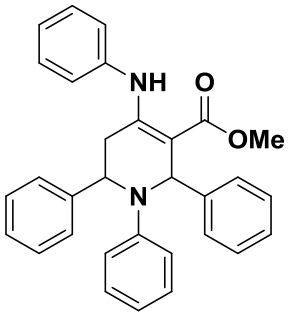 **(12d)**	RT	5h	85%	200-202ºC

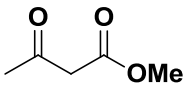 **6a**	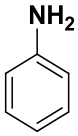 **7a**	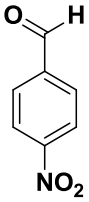 **8d**	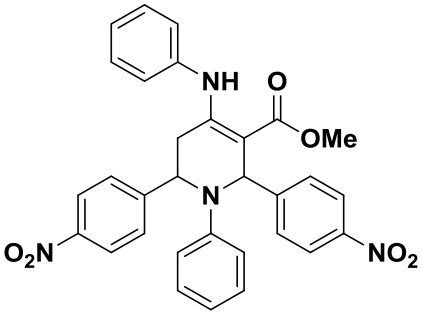 **(12e)**	50°C	9h	80%	255-256ºC
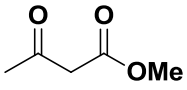 **6a**	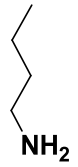 **7b**	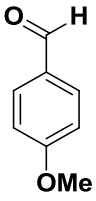 **8a**	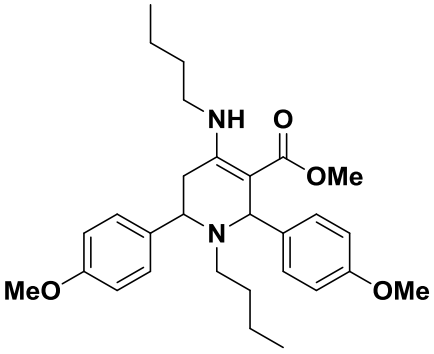 **(12f)**	50°C	12h	63%	150-151ºC

Characterization Data:

Compound 12a: The structure of compound **12a** was confirmed from its spectroscopic and analytical data (Fig. S21-S22, ESI†). ^{1}H NMR (500 MHz, $CDCl_3$, ppm) δ = 10.28 (s, 1H), 7.25 (d, *J* = 12Hz, 2H), 7.11-7.00 (m, 7H), 6.84 (d, *J* = 12Hz, 4H), 6.70 (t, *J* = 12Hz, 1H), 6.53 (d, *J* =12Hz, 2H), 6.34-6.29 (m, 3H), 5.14-5.07 (m, 1H), 3.93 (s, 3H), 3.75 (s, 3H), 3.71(s, 3H), 2.85 (dd, *J* = 10Hz, 1H), 2.78 (dd, *J* = 10 Hz, 1H). ^{13}C NMR (125 MHz, $CDCl_3$, ppm) δ = 168.71, 158.88, 158.01, 156.28, 147.05, 129.26, 128.92, 128.83, 128.79, 126.54, 126.30, 125.81, 125.62, 115.98, 114.14, 112.88, 98.09, 57.91, 54.91, 51.60, 50.98, 33.65. ESI-MS mass spectrum of compound **12a** showed a parent ion peak, m/z = 521.21 $[M+H]^+$. Elemental analysis: Calculated for $C_{32}H_{32}N_2O_4$: C 76.13; H 6.20; N 5.38; Found: C 76.11%; H 6.20%; N 5.37%.

Compound 12b: The structure of compound **12b** was confirmed from its spectroscopic and analytical data (Fig. S10-S20, ESI†). ^{1}H NMR (500 MHz, $CDCl_3$, ppm) δ = 10.23 (s, 1H), 7.22 (d, *J* = 10Hz, 2H) 7.01-6.98 (m, 11H), 6.55 (t, *J* = 5 Hz, 1H), 6.49 (d, *J* = 10 Hz, 2H), 6.40 (s, 1H), 6.24 (d, *J* = 10Hz, 2H), 5.05-4.92 (m, 1H), 4.41-4.37 (m, 1H), 4.29-4.27 (m, 1H), 2.96 (dd, *J* = 10Hz, 1H), 2.78 (dd, *J* = 12.5, 1H), 2.51 (s, 3H), 2.50 (s, 3H), 1.39 (t, *J* = 7.5 Hz, 3H). ^{13}C NMR (125 MHz, $CDCl_3$, ppm) δ = 168.60, 156.28, 147.05, 140.93, 139.66, 137.93, 136.60, 129.25, 128.92, 128.79, 126.54, 126.30, 125.81, 125.62, 115.98, 112.88, 98.09, 57.91, 54.91, 50.98, 33.65, 21.10, 21.0, 14.14. ESI-MS mass spectrum of compound **12b** showed a parent ion peak, m/z = 503.25 $[M+H]^+$. Elemental analysis: Calculated for $C_{34}H_{34}N_2O_2$: C 81.24; H 6.82; N 5.57; Found: C 81.22%; H 6.83%; N 5.56%.

Compound 12c: The structure of compound **12c** was confirmed from its spectroscopic and analytical data (Fig. S17-S18, ESI†). ^{1}H NMR (500 MHz, $CDCl_3$, ppm) δ = 10.24 (s, 1H), 7.19 (d, *J* = 10 Hz, 2H, ArH), 7.08-7.03 (m, 11H, ArH), 6.56 (t, *J* = 10 Hz, 1H), 6.52 (d, *J* = 10Hz, 2H), 6.39 (s, 1H), 6.31-6.29 (m, 2H, ArH), 5.11 (s, 1H), 3.92 (s, 3H), 2.88 (dd, *J* = 10 Hz, 1H), 2.75 (dd, *J* = 10 Hz, 1H), 2.33 (s, 3H), 2.32 (s, 3H). ^{13}C NMR (125 MHz, $CDCl_3$, ppm) δ = 168.60, 156.28, 147.05, 140.93, 139.67, 137.93, 136.60, 135.77, 128.92, 128.83, 128.79, 125.81, 115.98, 112.89, 98.09, 57.91, 54.91, 50.98, 33.65, 21.11, 21.02). ESI-MS mass spectrum of compound **12c** showed a parent ion peak, m/z = 489.25 $[M+H]^+$. Elemental analysis: Calculated for $C_{33}H_{32}N_2O_2$: C 81.12; H 6.60; N 5.73; Found: C 81.11%; H 6.61%; N 5.71%.

Compound 12d: The structure of compound **12d** was confirmed from its spectroscopic and analytical data (Fig. S23-S24, ESI†). ^{1}H NMR (500 MHz, $CDCl_3$, ppm) δ = 10.05 (s, 1H), 7.20-7.18 (m, 8H), 7.16 (d, *J* = 10 Hz, 2H), 7.07-7.03 (m, 5H), 6.91 (d, *J* = 10 Hz, 1H), 6.64 (d, *J* = 10Hz, 2H), 6.58 (s, 1H), 6.29 (d, *J* = 10Hz, 2H), 5.37-5.35 (m, 1H), 3.51 (s, 3H), 2.35 (dd, *J* = 10 Hz, 1H), 2.32 (dd, *J* = 10 Hz, 1H). ^{13}C NMR (125 MHz, $CDCl_3$, ppm) δ = 168.70, 156.52, 147.04, 144.46, 142.65, 137.92, 129.25, 128.91, 128.82, 128.78, 125.80, 116.80, 113.67, 98.08, 58.38, 55.34, 51.37, 33.64. ESI-MS mass spectrum of compound **12d** showed a parent ion peak, m/z = 461.30 $[M+H]^+$. Elemental analysis: Calculated for $C_{31}H_{28}N_2O_2$: C 80.84; H 6.13; N 6.08; Found: C 80.82%; H 6.11%; N 6.07%.

Compound 12e: The structure of compound **12e** was confirmed from its spectroscopic and analytical data (Fig. S25-S26, ESI†). ^{1}H NMR (500 MHz, $CDCl_3$, ppm) δ =10.72 (s, 1H), 8.60 (d, *J* = 5 Hz, 1H), 8.37 (t, *J* = 10Hz, 4H), 8.27-8.10 (m, 4H), 7.66 (t, *J* = 10 Hz, 2H), 7.57 (t, *J* = 10 Hz, 2H), 7.46 (t, *J* = 10 Hz, 2H), 6.92-6.73 (t, *J* = 10 Hz, 4H), 5.75-5.49 (m, 1H), 2.42-2.40 (m, 1H), 2.39-2.31 (m, 1H). ^{13}C NMR (125 MHz, $CDCl_3$, ppm) δ = 168.77, 155.38, 151.06, 149.94, 147.21, 146.14, 145.32, 137.14, 129.50, 129.21, 128.69, 127.32, 127.02, 126.26, 125.43, 123.53, 118.62, 113.43, 96.24, 57.23, 55.32, 51.77, 33.25. ESI-MS mass spectrum of compound **12e** showed a parent ion peak, m/z = 551.16 $[M+H]^+$. Elemental analysis: Calculated for $C_{31}H_{26}N_4O_6$: C 67.63.13; H 4.76; N 10.18; Found: C 67.62%; H 4.75%; N 10.18%.

Compound 12f: The structure of compound **12f** was confirmed from its spectroscopic and analytical data (Fig. S27-S28, ESI†). ^{1}H NMR (500 MHz, $CDCl_3$, ppm) δ = 9.89 (s, 1H), 7.85 (d, *J* = 15 Hz, 2H), 7.13 (d, *J* = 15 Hz, 2H), 7.01 (d, *J* = 15 Hz, 2H), 6.82 (d, *J* = 15Hz, 2H), 4.01 (s, 1H), 3.93 (dd, *J* = 15 Hz, 1H), 3.78 (s, 3H), 3.57 (s, 3H), 3.40 (s, 3H), 3.04-3.00 (m, 2H), 2.71 (dd, 1H), 2.49 (dd, *J* = 15 Hz, 1H), 1.58-1.25 (m, 10H), 0.83 (t, *J* = 10 Hz, 3H), 0.70 (t, *J* =10 Hz, 3H). ^{13}C NMR (500 MHz, $CDCl_3$, ppm) δ = 174.22, 158.97, 142.38, 139.62, 136.28, 132.00, 130.10, 128.78, 127.79, 88.50, 58.79, 57.33, 55.19, 52.62, 44.33, 42.01, 41.67, 28.67, 28.10, 23.49, 20.94, 20.22, 14,36, 13.51. ESI-MS mass spectrum of compound **12f** showed a parent ion peak, m/z = 481.18 $[M+H]^+$. Elemental analysis: Calculated for $C_{29}H_{40}N_2O_4$: C 72.37; H 8.39; N 5.83; Found: C 72.36%; H 8.38%; N 5.82%.

Intermediate 9: The structure of intermediate **9** was confirmed from its spectroscopic data (Fig. S29A, ESI†). ^{1}H NMR (500 MHz, $CDCl_3$, ppm) δ =10.36 (s, 1H), 7.34-7.29 (m, 2H), 7.17-7.09 (m, 2H), 6.76-6.66 (m, 1H), 4.70 (s, 1H, -NH), 3.68 (s, 3H), 1.98 (s, 3H).

Intermediate 10: The structure of intermediate **10** was confirmed from its spectroscopic data (Fig. S29B, ESI†). ^{1}H NMR (500 MHz, $CDCl_3$, ppm) δ = 8.32 (d, *J* = 5 Hz, 2H, ArH), 7.80 (s, 1H), 7.35-7.23 (m, 2H, ArH), 7.19-7.12 (m, 1H, ArH), 7.09-7.01 (m, 2H, ArH), 6.93-6.90 (d, *J* = 15 Hz, 2H, ArH), 3.79 (s, 3H), 3.62 (s, 3H), 1.93 (s, 3H).

Intermediate 11: The structure of intermediate **11** was confirmed from its spectroscopic data (Fig. S30, ESI†). ^{1}H NMR (500 MHz, $CDCl_3$, ppm) δ = 9.91 (s, 1H, HC=N), 8.42-8.36 (m, 1H, ArH) 7.86-7.83 (t, *J* = 15 Hz, 2H, ArH), 7.41-7.38 (d, *J* = 15 Hz, 2H, ArH), 7.21 (d, 2H, ArH), 6.99 (d, 2H, ArH), 3.87 (s, 3H).

Compound 13: The structure of intermediate **13** was confirmed from its spectroscopic data (Fig. S31, ESI†). ^{1}H NMR (500 MHz, $CDCl_3$, ppm) δ = 7.34 (d, *J* = 5Hz, 2H, ArH), 7.30 (s, 2H, ArH), 7.25 (t, *J* = 5Hz, 2H), 7.18-7.12 (m, 1H), 6.78-6.73 (m, 1H), 6.70-6.63 (m, 2H), 4.73 (d, *J* = 10Hz, 1H), 4.59 (d, J = 10Hz, 1H), 2.81 (t, *J* = 5Hz, 2H), 1.94-1.84 (m, 4H), 1.80-1.73 (m, 2H). ESI-MS mass spectrum of compound **13** showed a parent ion peak, m/z = 313.16 [M].

Fig. S21A: ^{1}H NMR Spectra ($CDCl_3$, 500 MHz, ppm) of compound 12a:

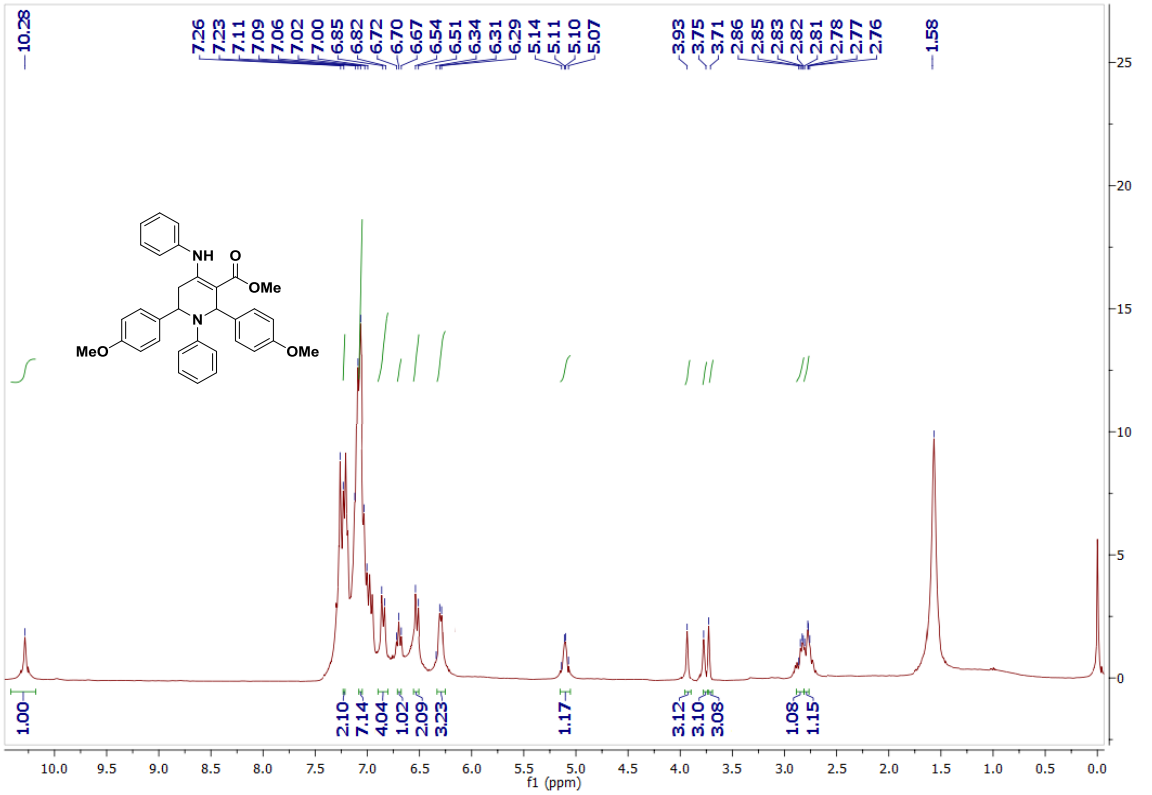

Fig. S21B: ^{13}C NMR Spectra ($CDCl_3$, 125 MHz, ppm) of compound 12a:

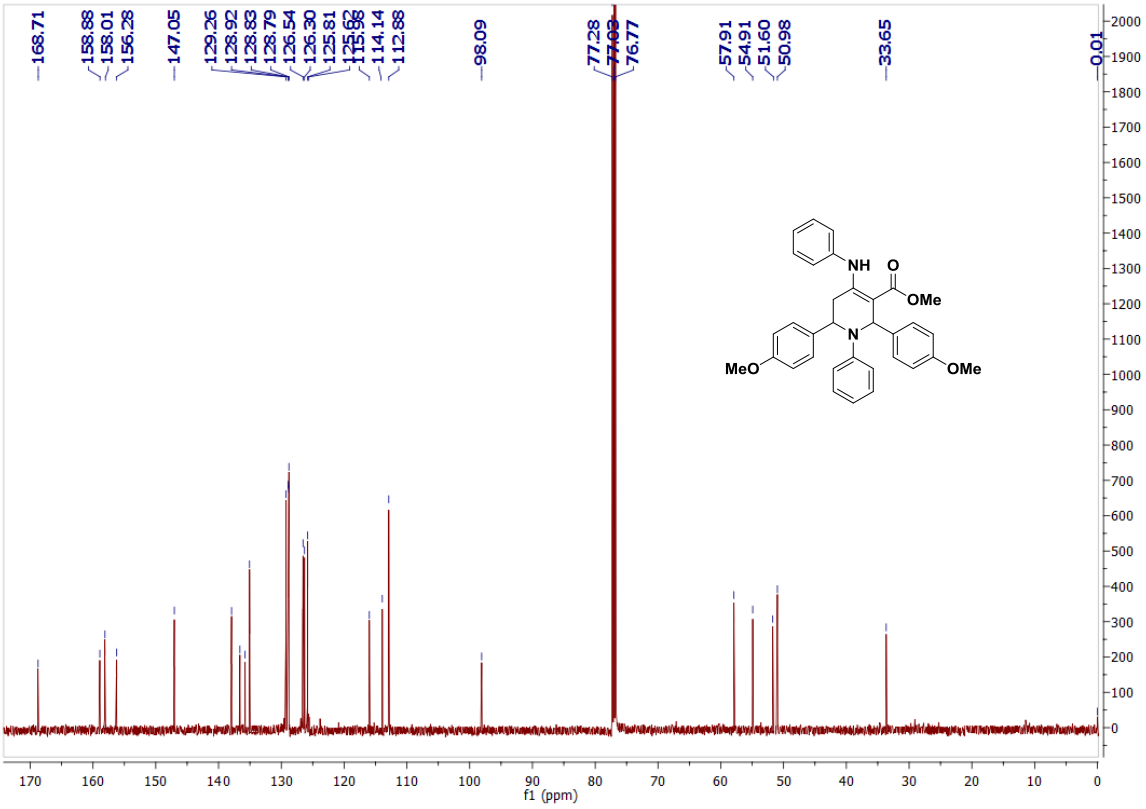

Fig. S22: ESI-MS spectrum of compound 12a:

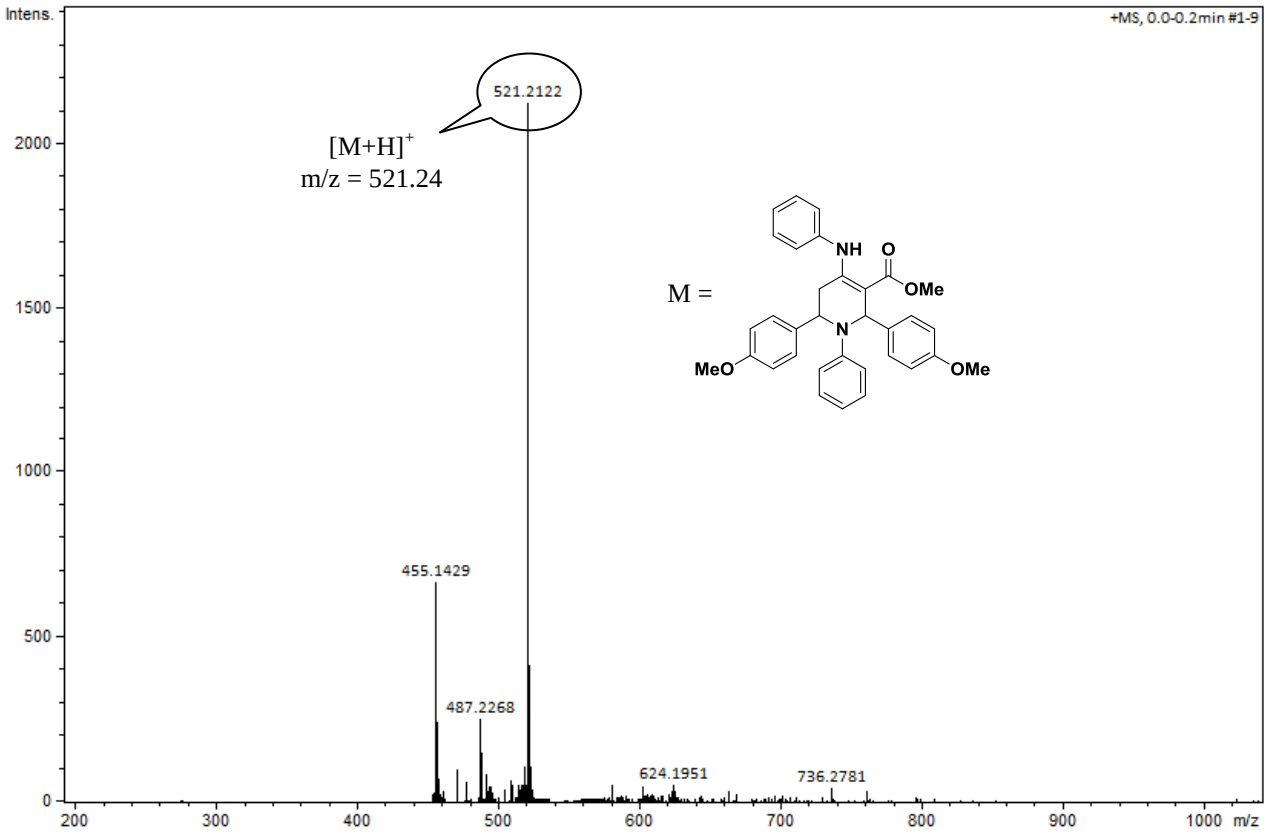

Fig. S19A: ^{1}H NMR Spectra ($CDCl_3$, 500 MHz, ppm) of compound 12b:

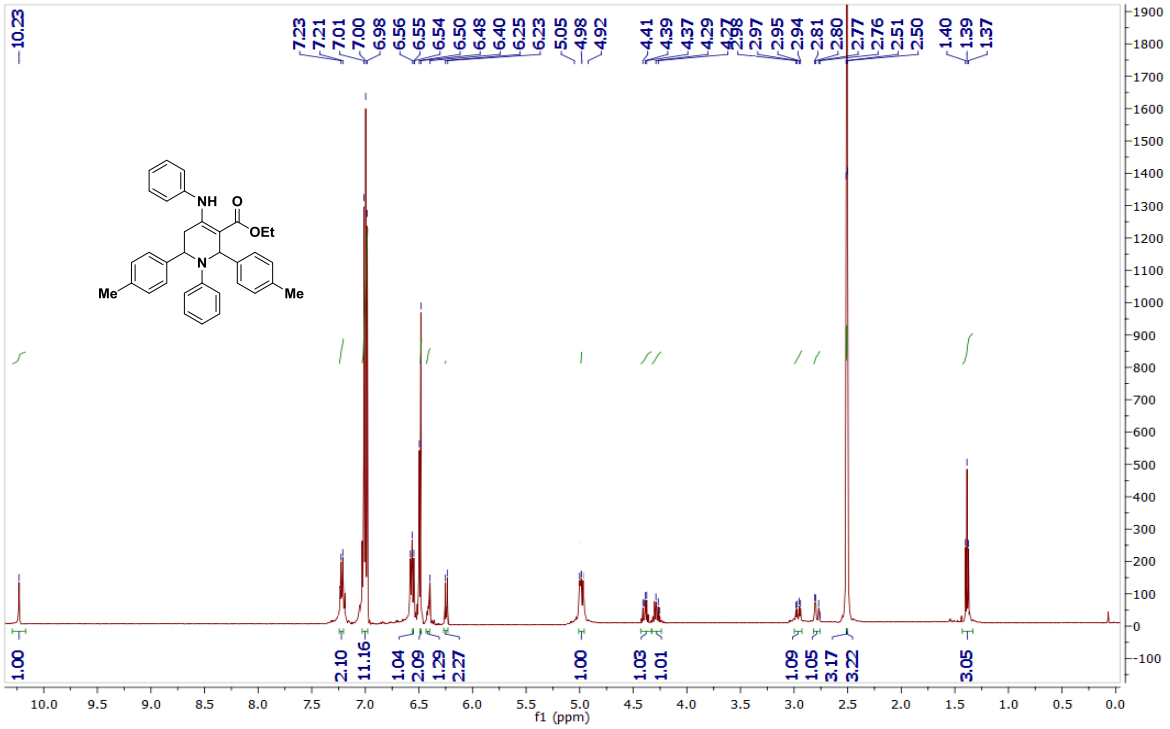

Fig. S19B: ^{13}C NMR Spectra ($CDCl_3$, 125 MHz, ppm) of compound 12b:

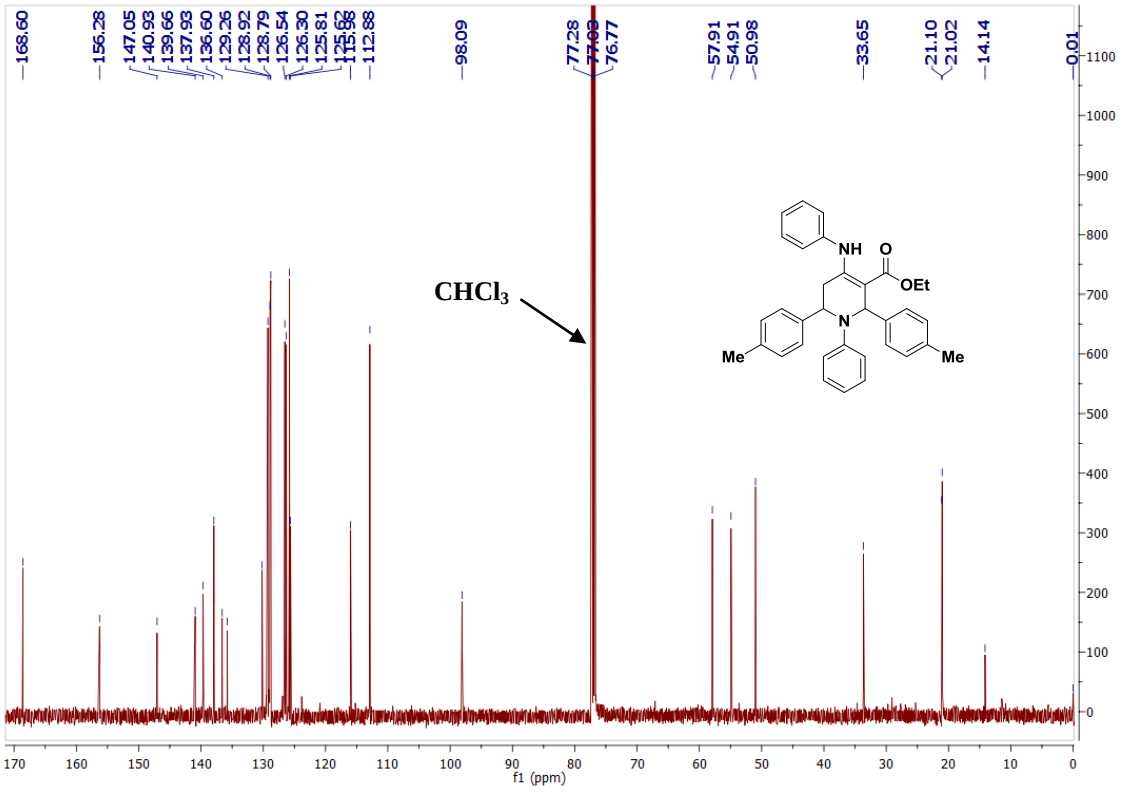

Fig. S20: ESI-MS spectrum of compound 12b:

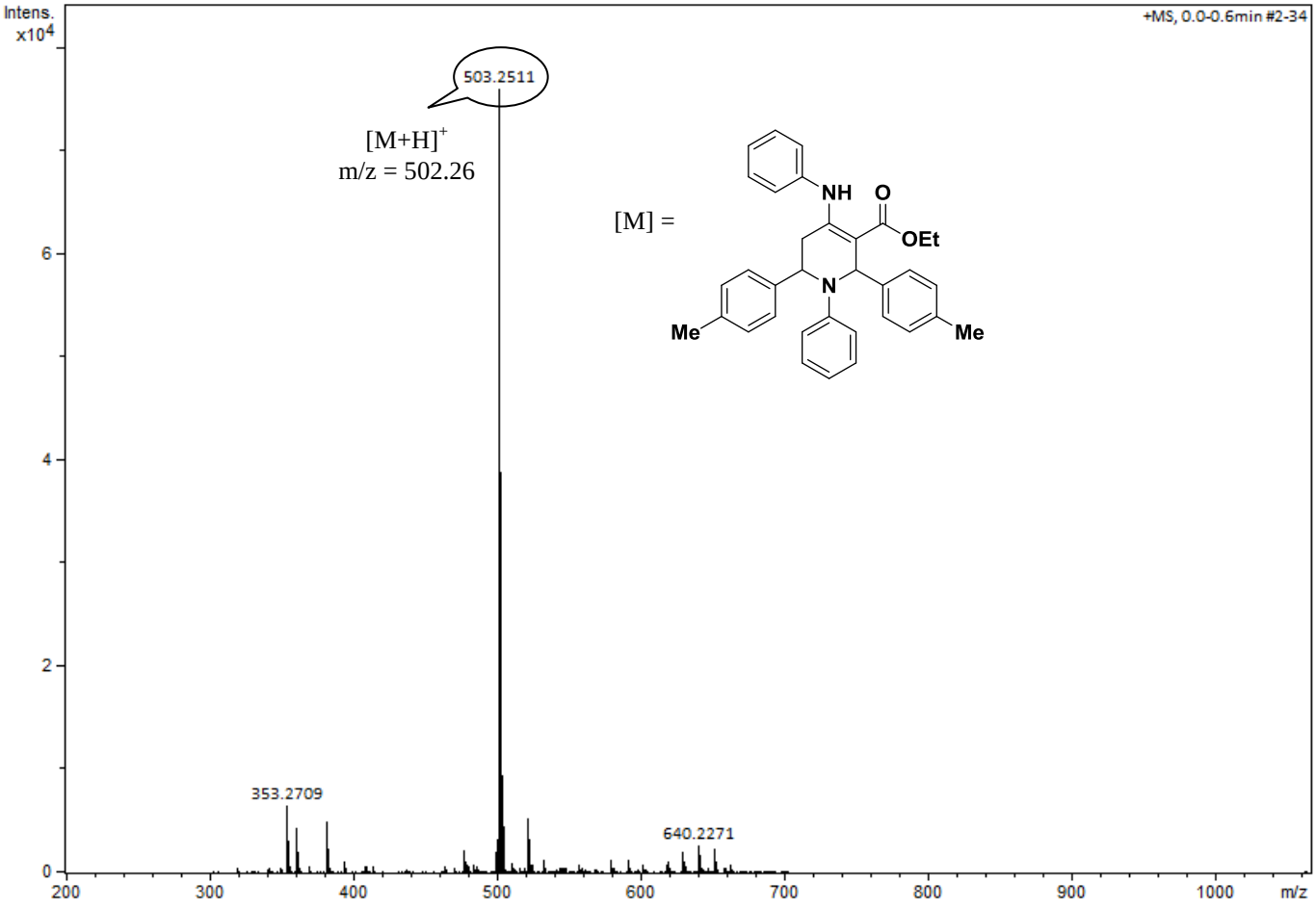

Fig. S17A: ^{1}H NMR Spectra ($CDCl_3$, 500 MHz, ppm) of compound 12c:

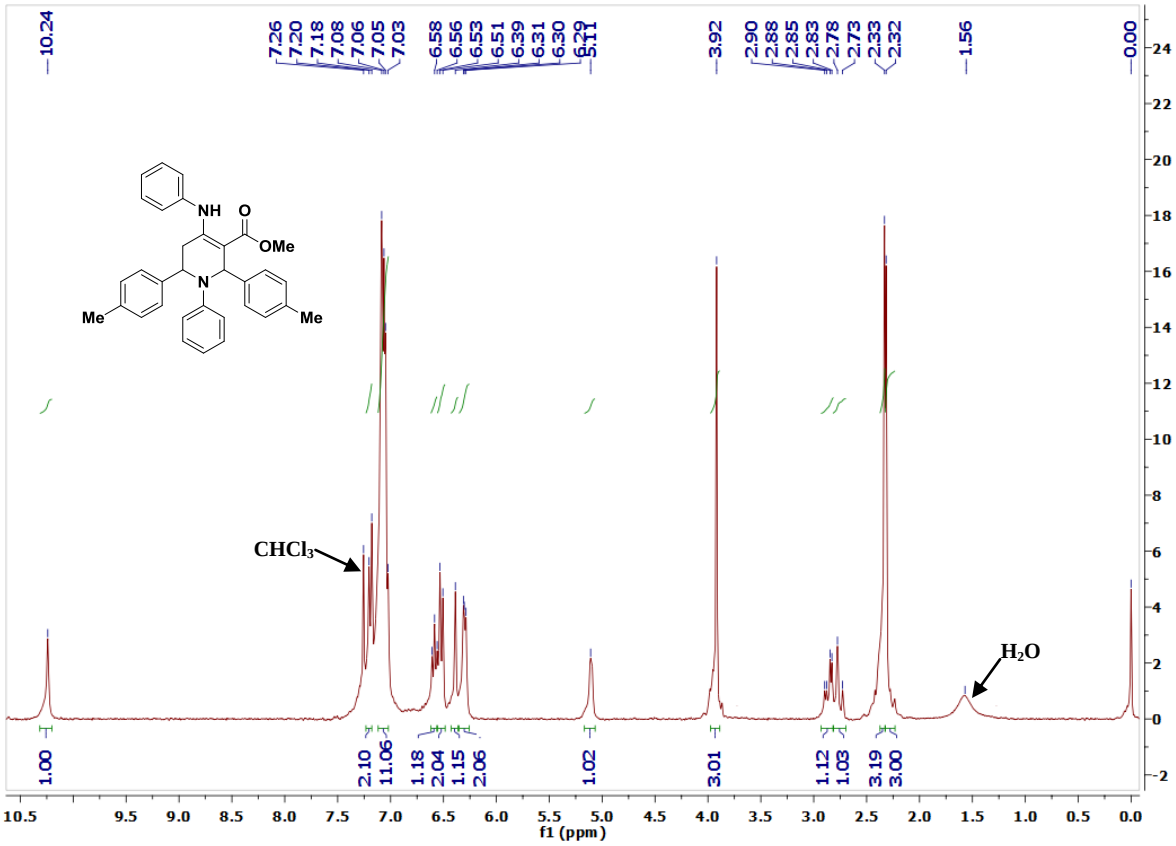

Fig. S17B: ^{13}C NMR Spectra ($CDCl_3$, 125 MHz, ppm) of compound 12c:

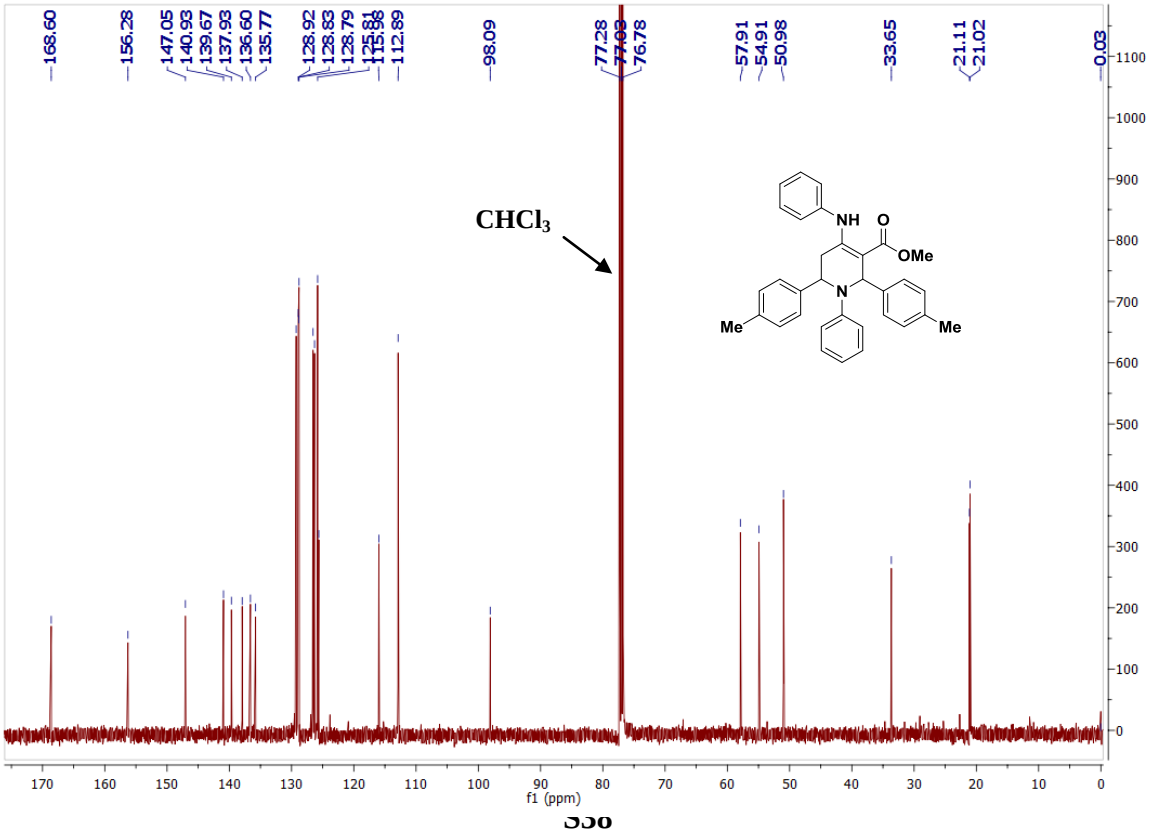

Fig. S18: ESI-MS spectrum of compound 12c:

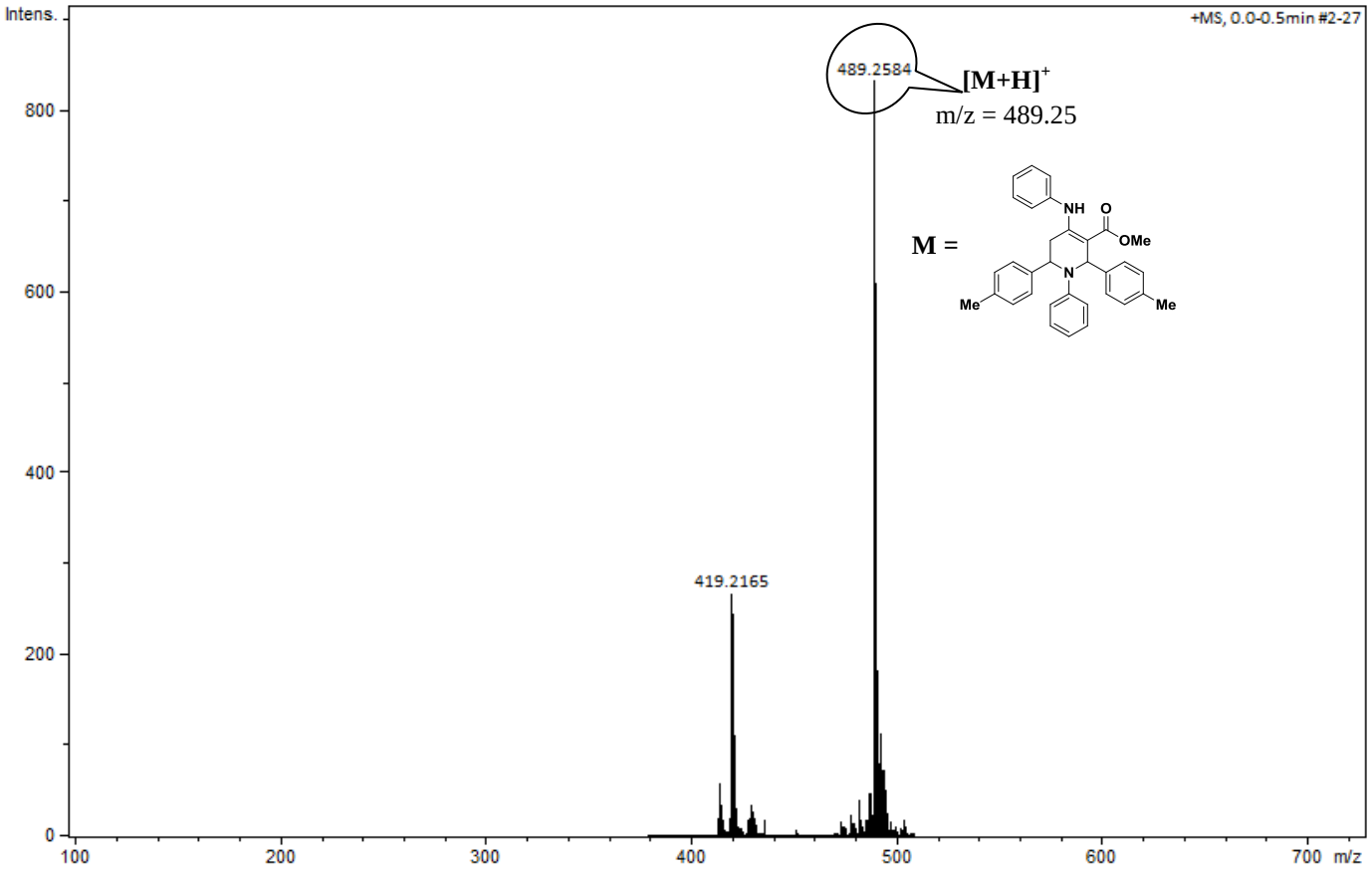

Fig. S23A: ^{1}H NMR Spectra ($CDCl_3$, 500 MHz, ppm) of compound 12d:

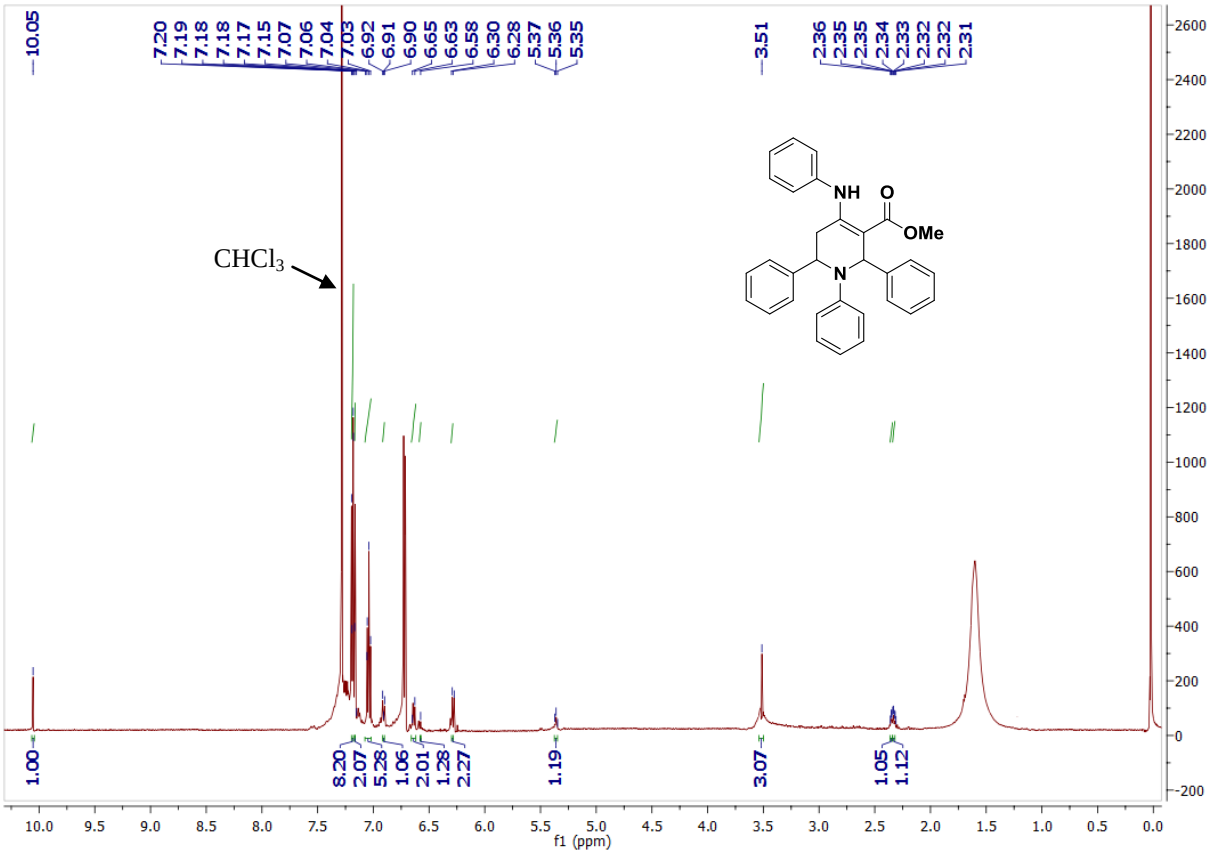

Fig. S23B: ^{13}C NMR Spectra ($CDCl_3$, 125 MHz, ppm) of compound 12d:

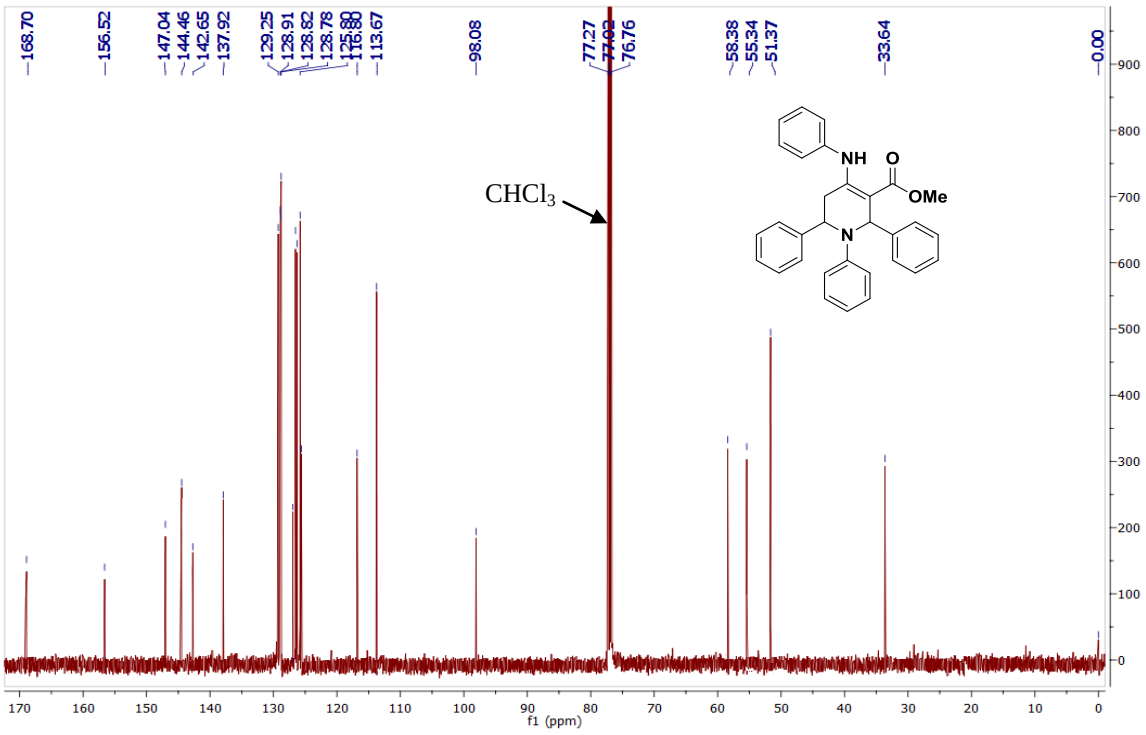

Fig. S24: ESI-MS spectrum of compound 12d:

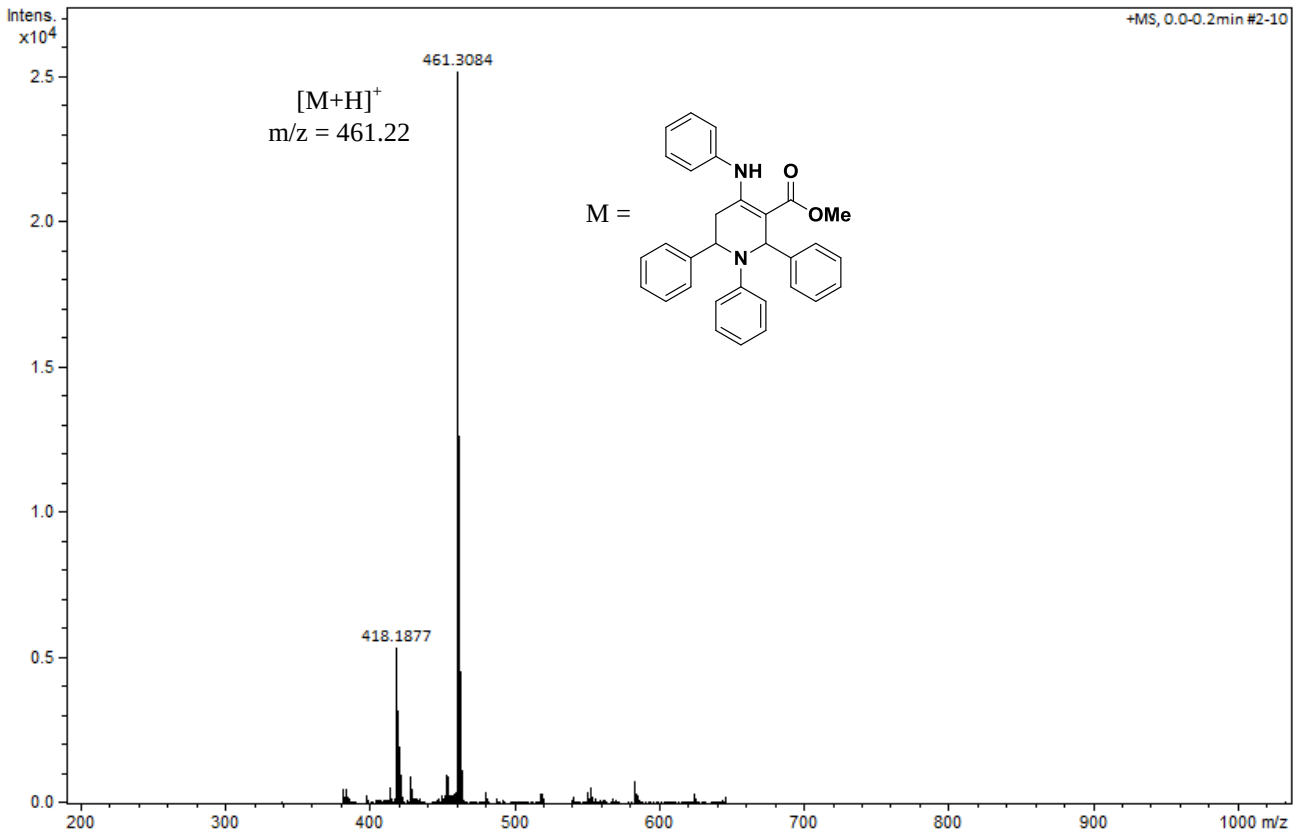

Fig. S25B: ^{13}C NMR Spectra ($CDCl_3$, 500 MHz, ppm) of compound 12e:

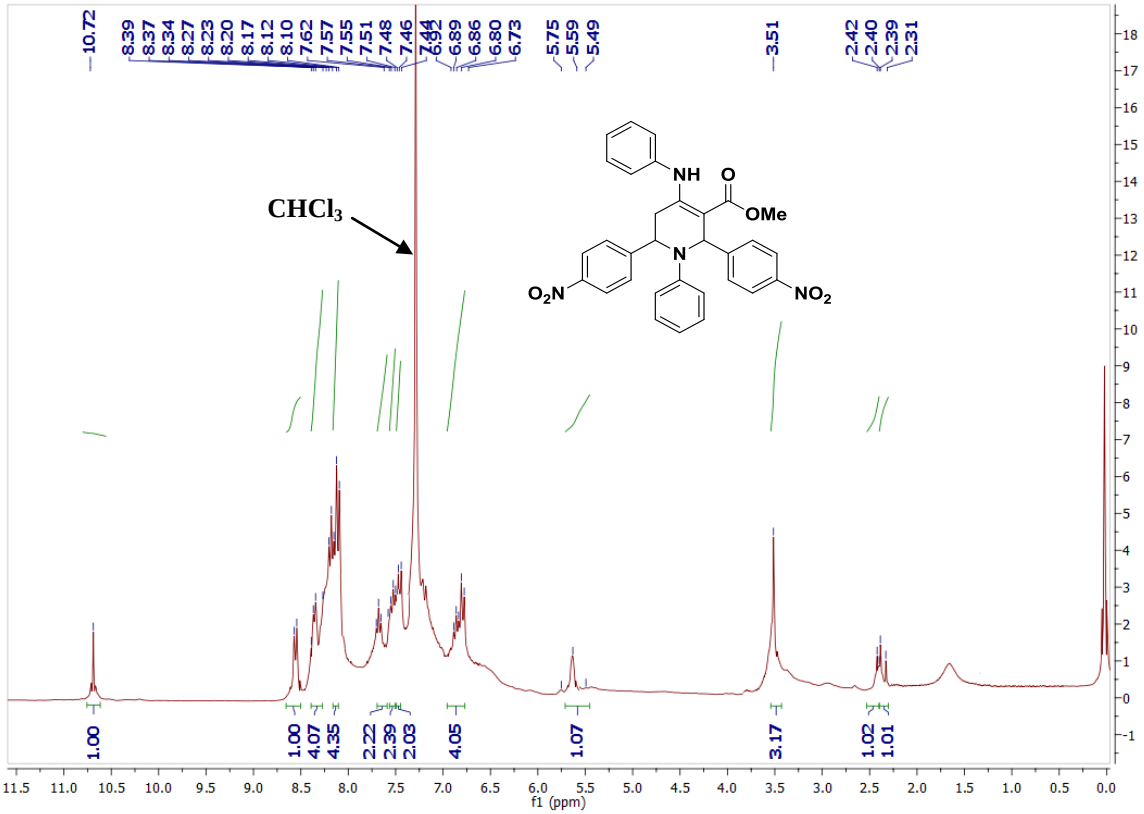

Fig. S25B: ^{13}C NMR Spectra ($CDCl_3$, 125 MHz, ppm) of compound 12e:

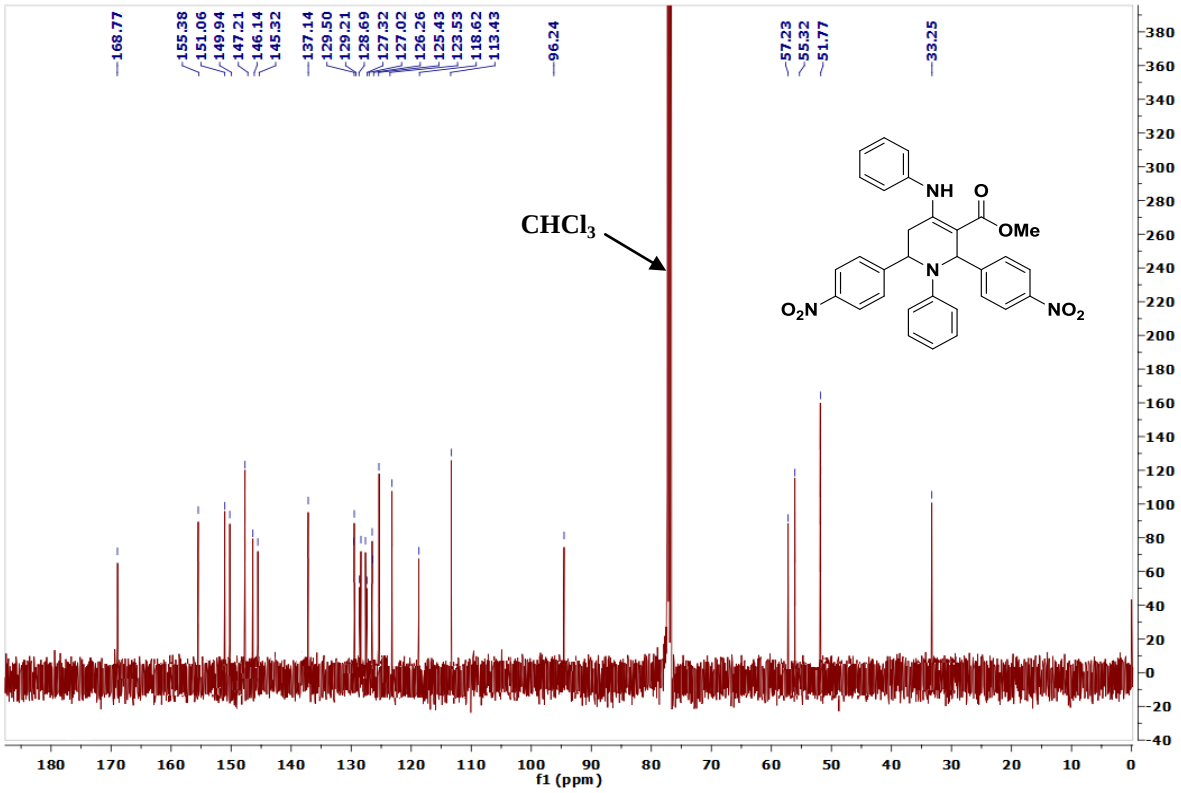

Fig. S26: ESI-MS spectrum of compound 12e:

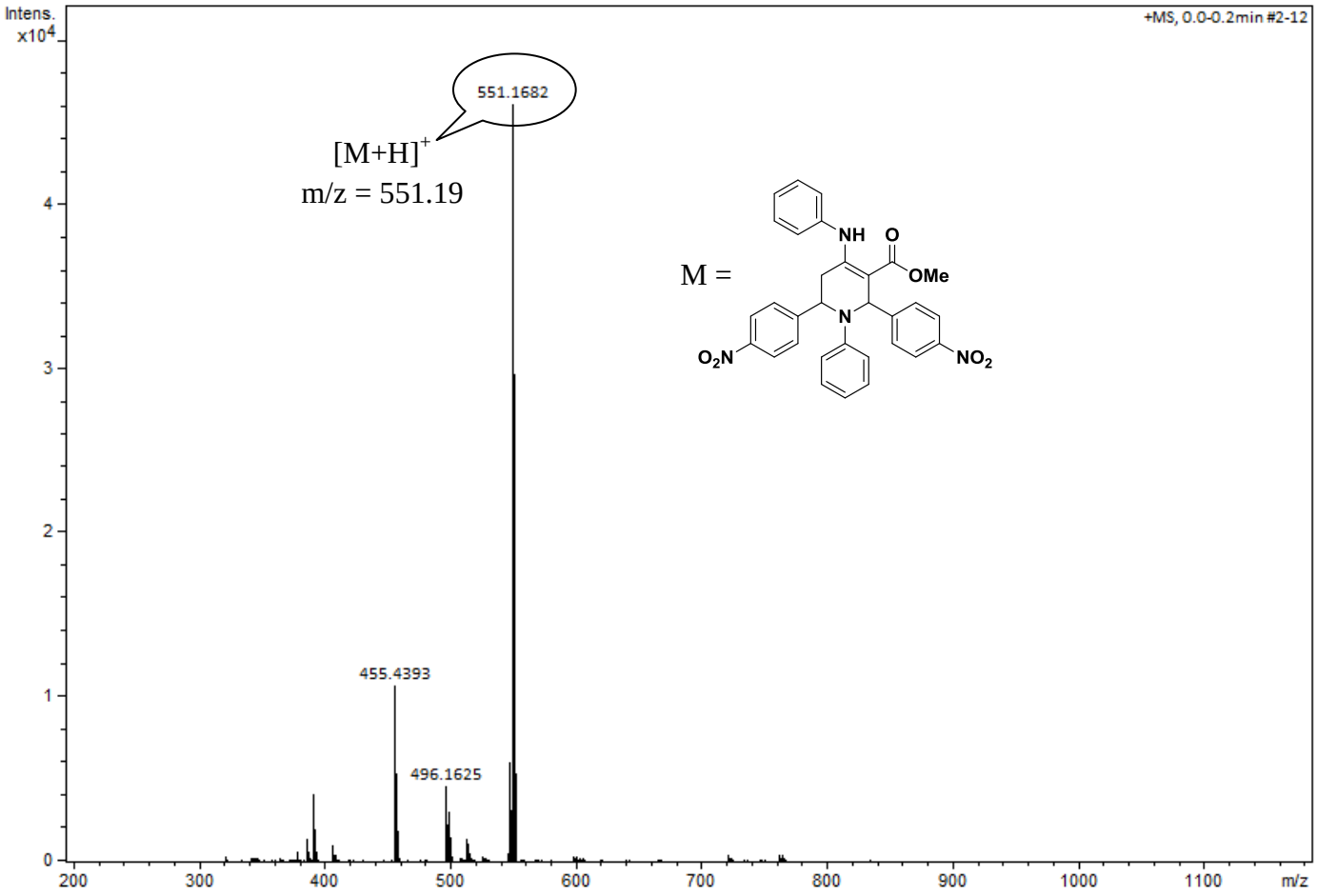

Fig. S27A: ^{1}H NMR Spectra ($CDCl_3$, 500 MHz, ppm) of compound 12f:

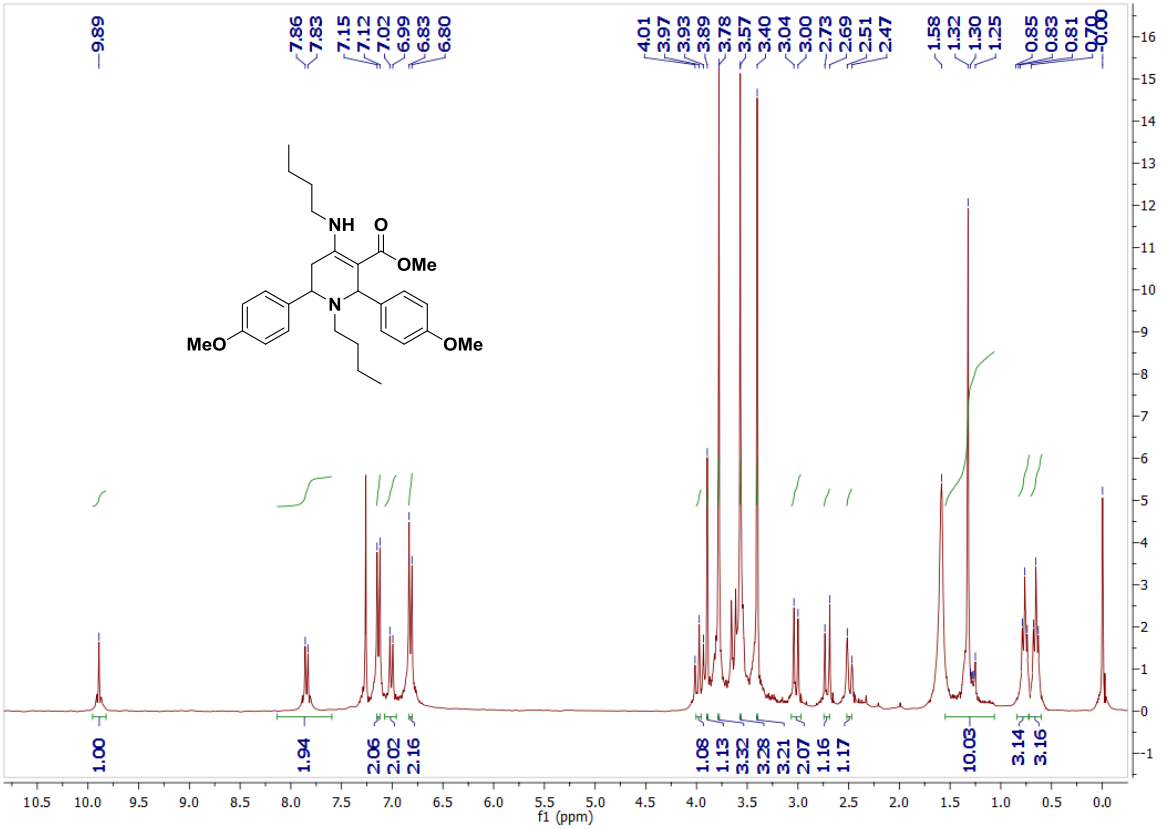

Fig. S27B: ^{13}C NMR Spectra ($CDCl_3$, 125 MHz, ppm) of compound 12f:

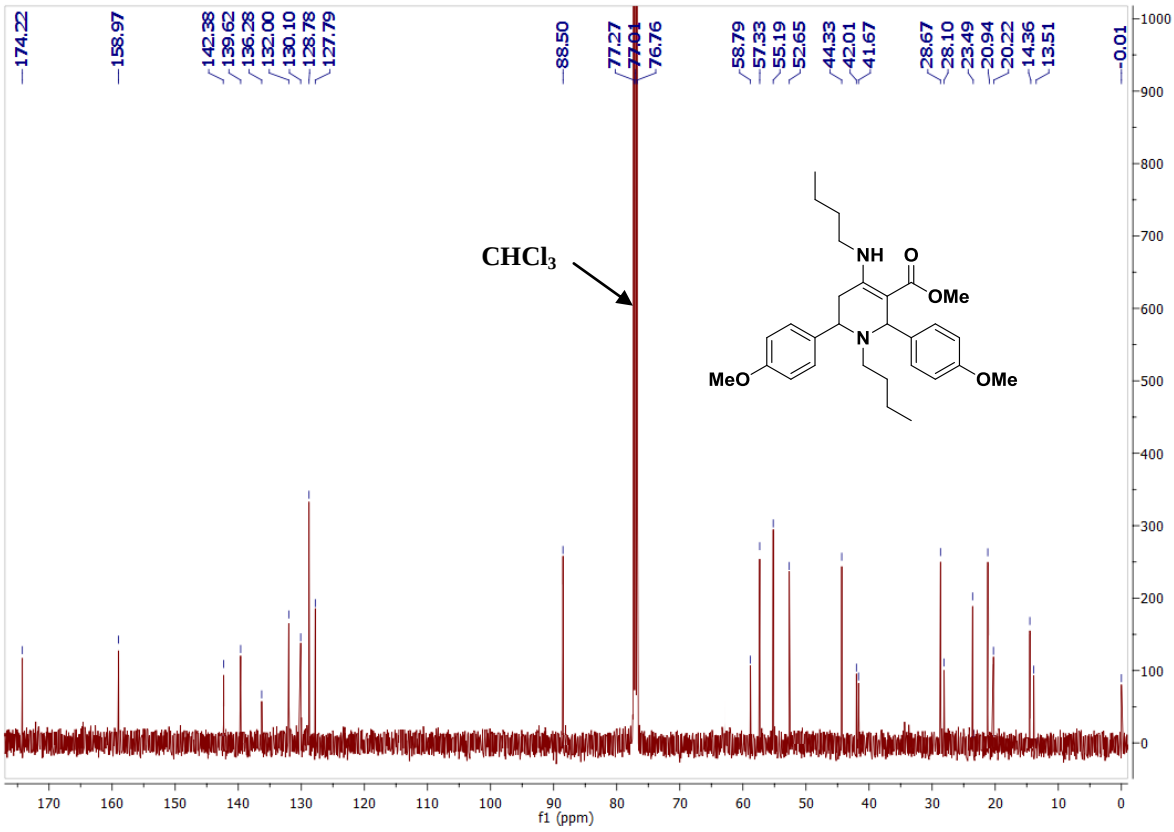

Fig. S28: ESI-MS spectrum of compound 12f:

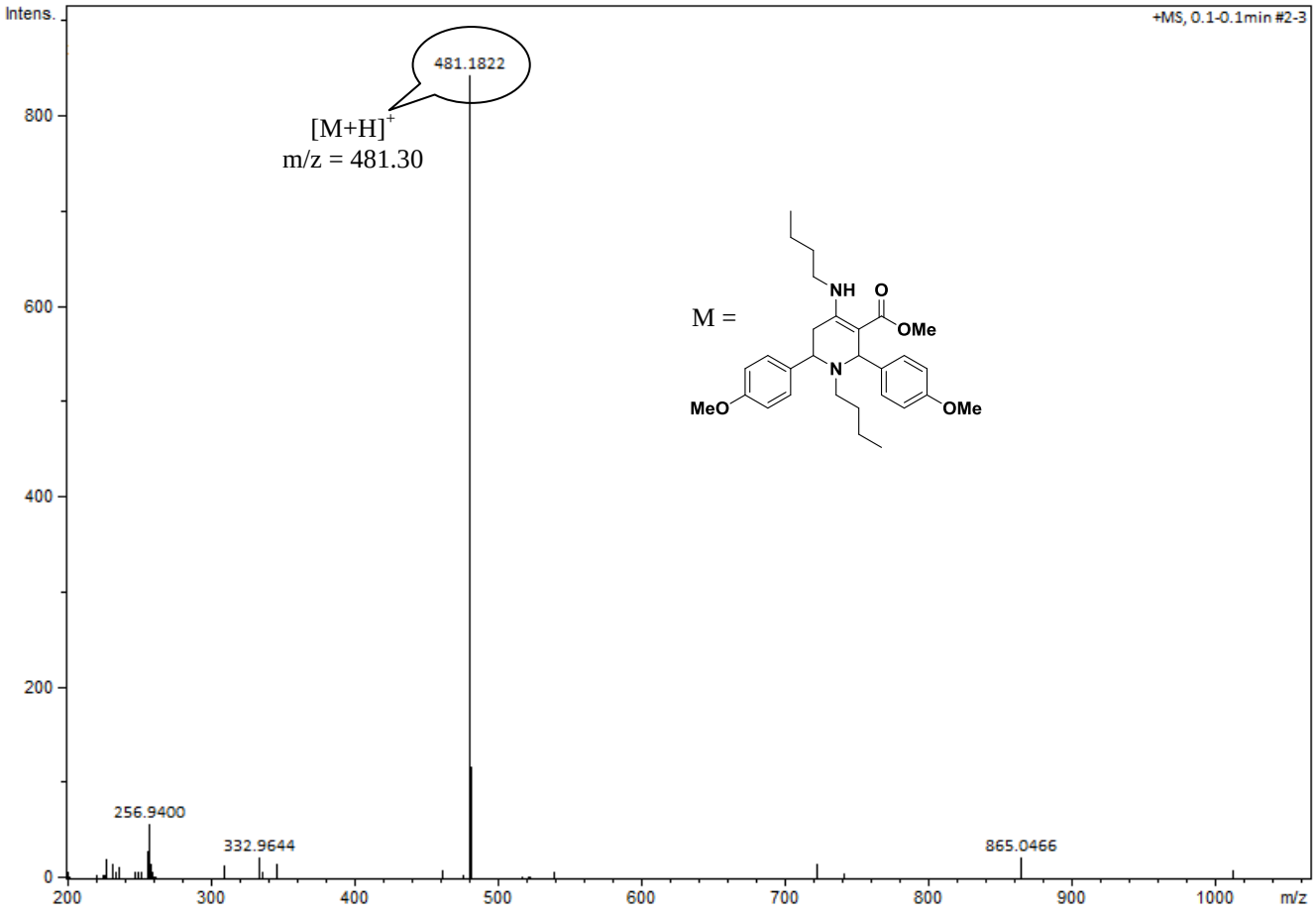

Fig. S29A: ^{1}H NMR Spectra ($CDCl_3$, 500 MHz, ppm) of compound intermediate 9 (12a):

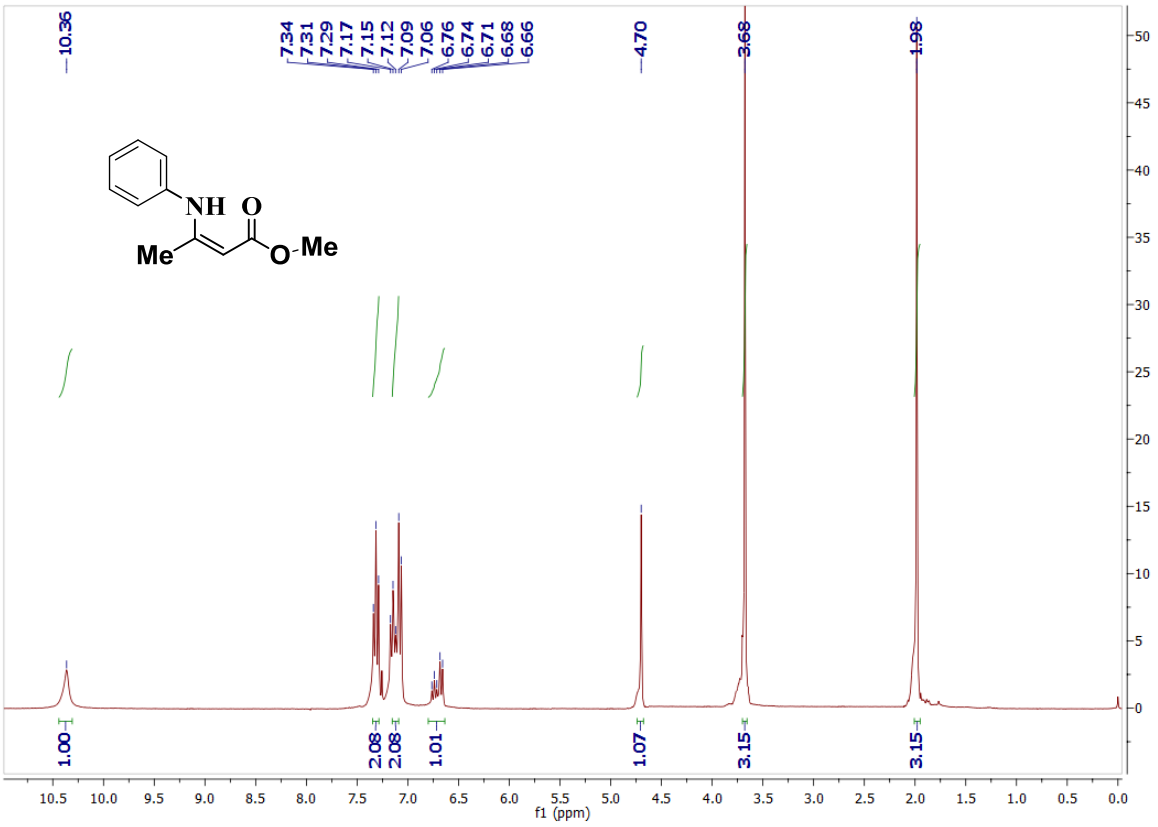

Fig. S29B: ^{1}H NMR Spectra ($CDCl_3$, 500 MHz, ppm) of intermediate 10 (12a):

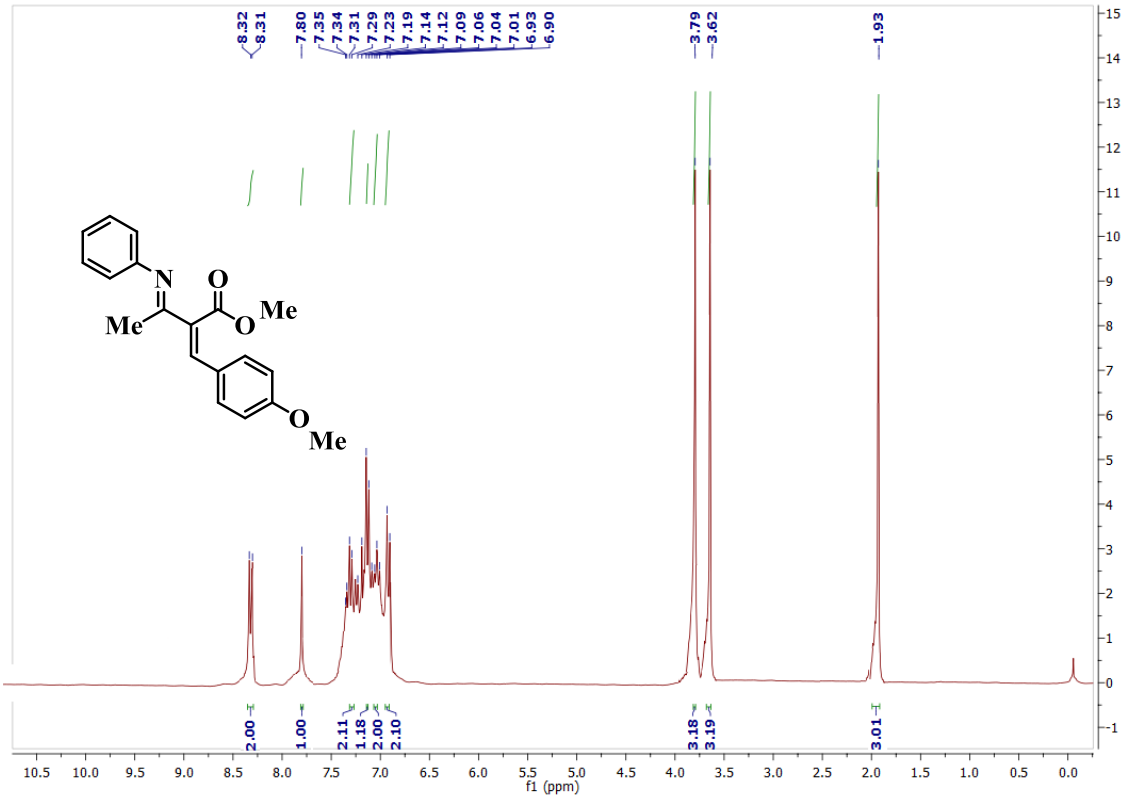

Fig. S30: ^{1}H NMR Spectra ($CDCl_3$, 500 MHz, ppm) of intermediate 11 (12a):

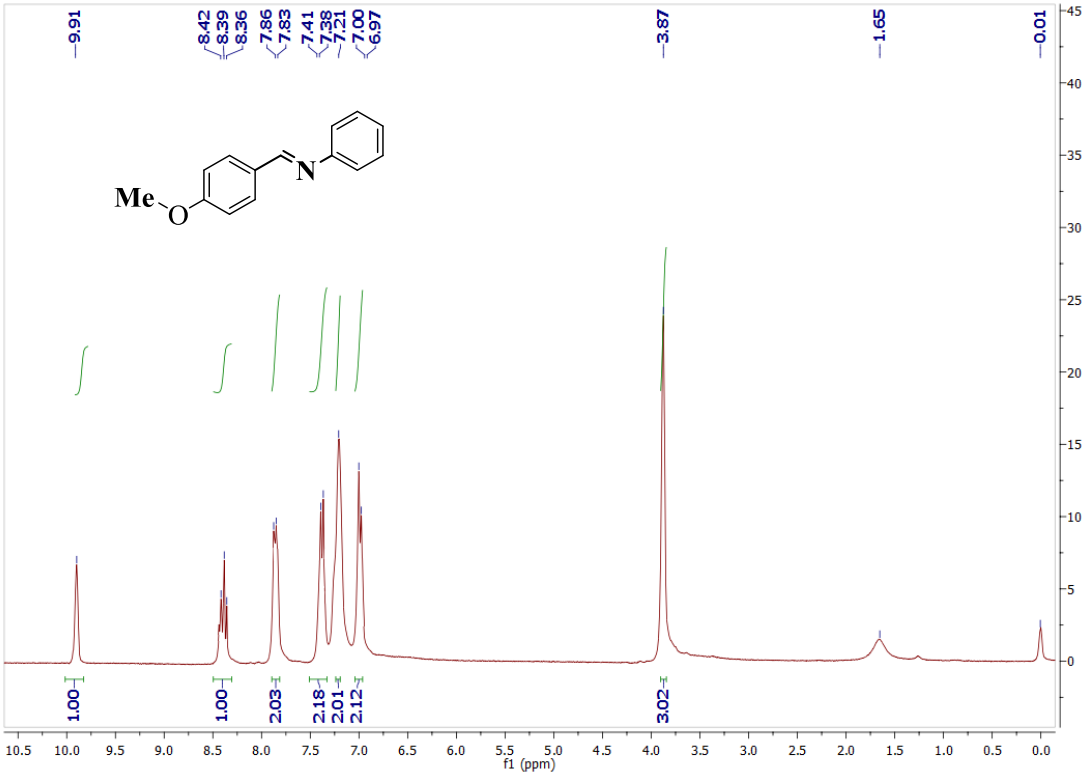

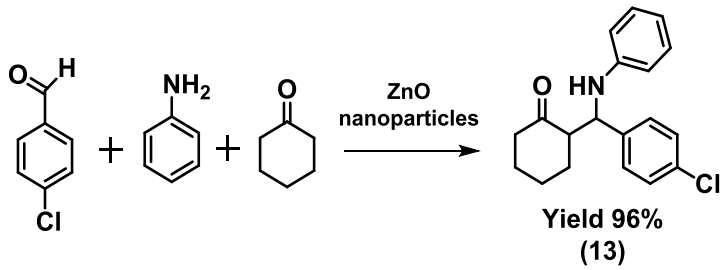

Scheme 3: Synthesis of β-amino ketones *via* three-component Mannich reaction by ZnO NPs.

Fig. S31A: ^{1}H NMR Spectra ($CDCl_3$, 500 MHz, ppm) of compound 13:

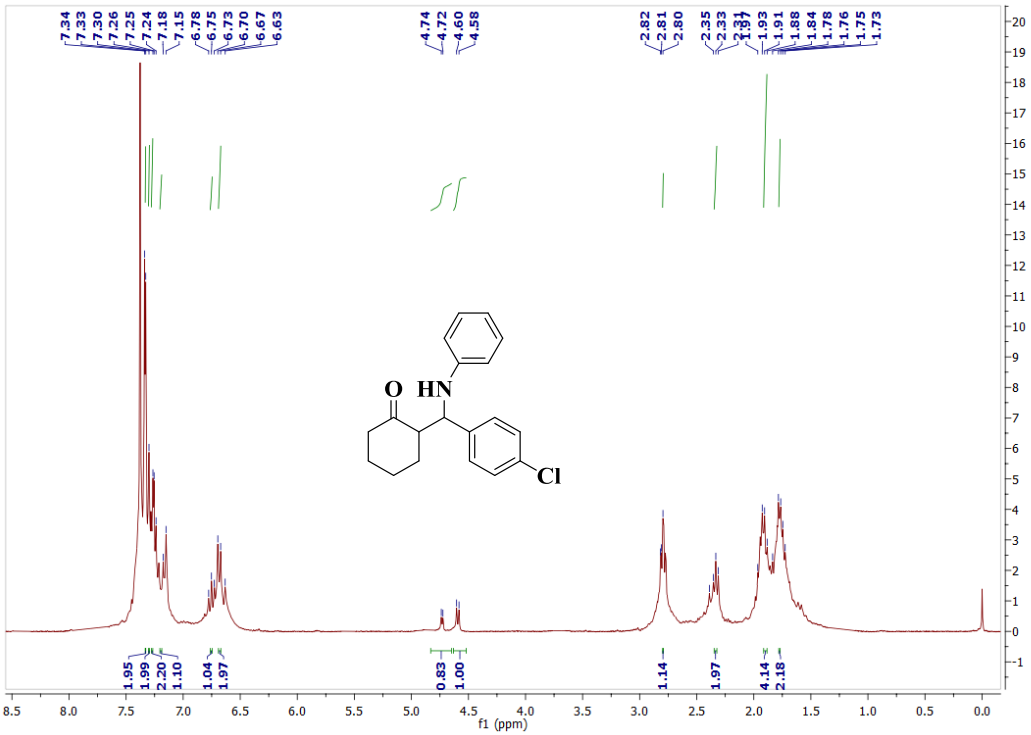

Fig. S31B: ESI-MS spectrum of compound 13:

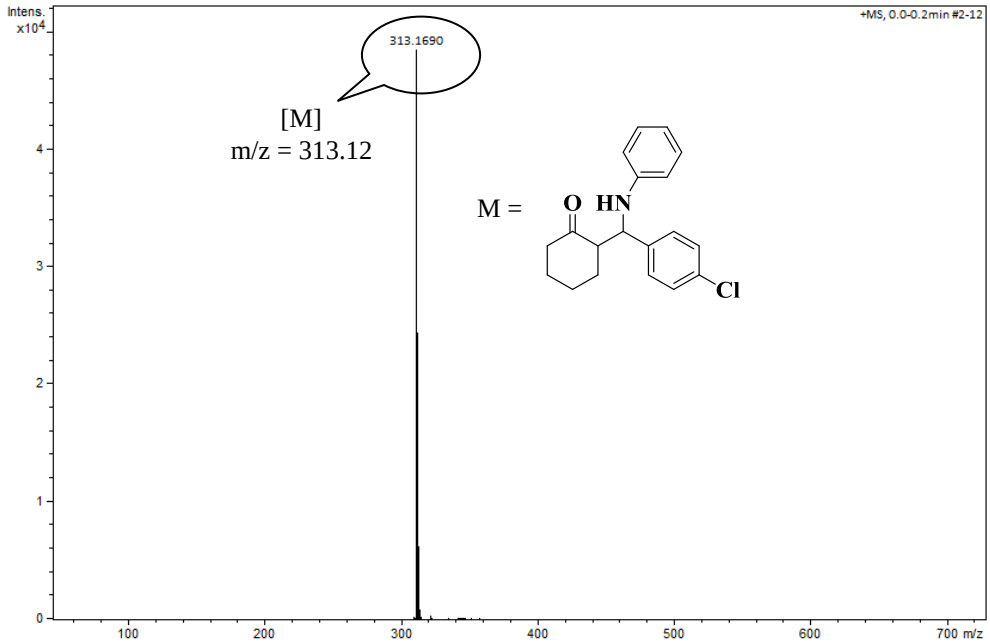

Fig. S32A: ^{1}H NMR Spectra ($CDCl_3$, 500 MHz, ppm) of compound 2a:

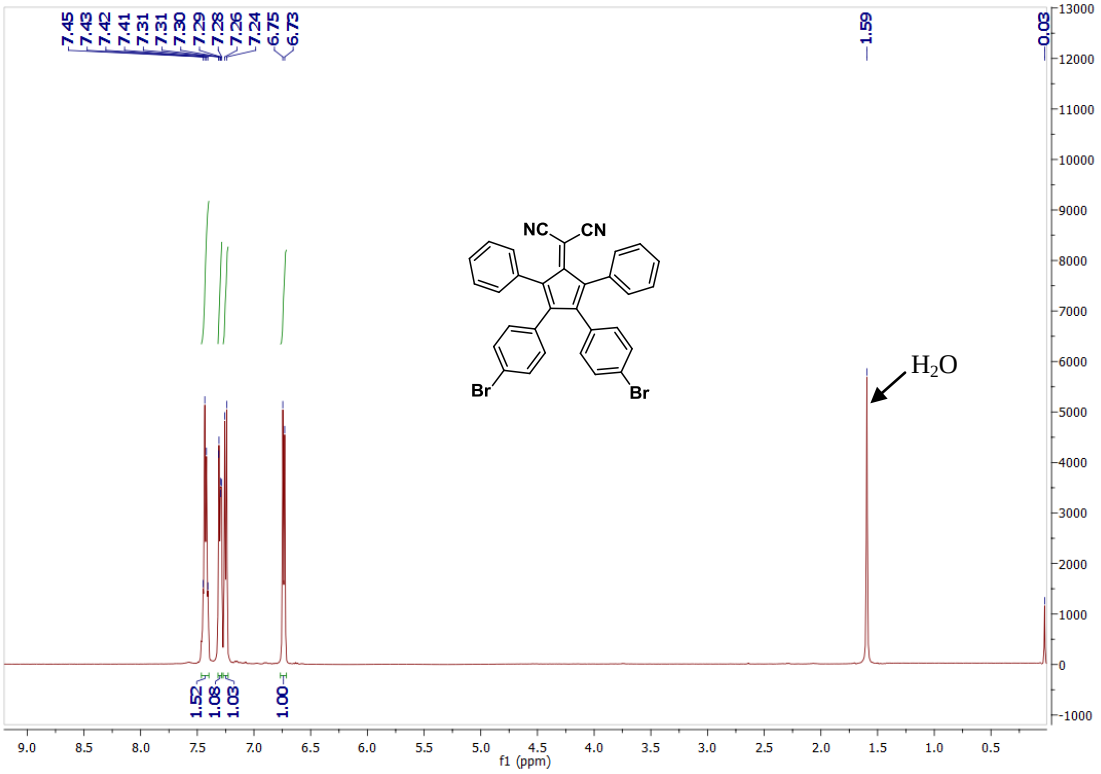

Fig. S32B: ^{13}C NMR Spectra ($CDCl_3$, 125 MHz, ppm) of compound 2a:

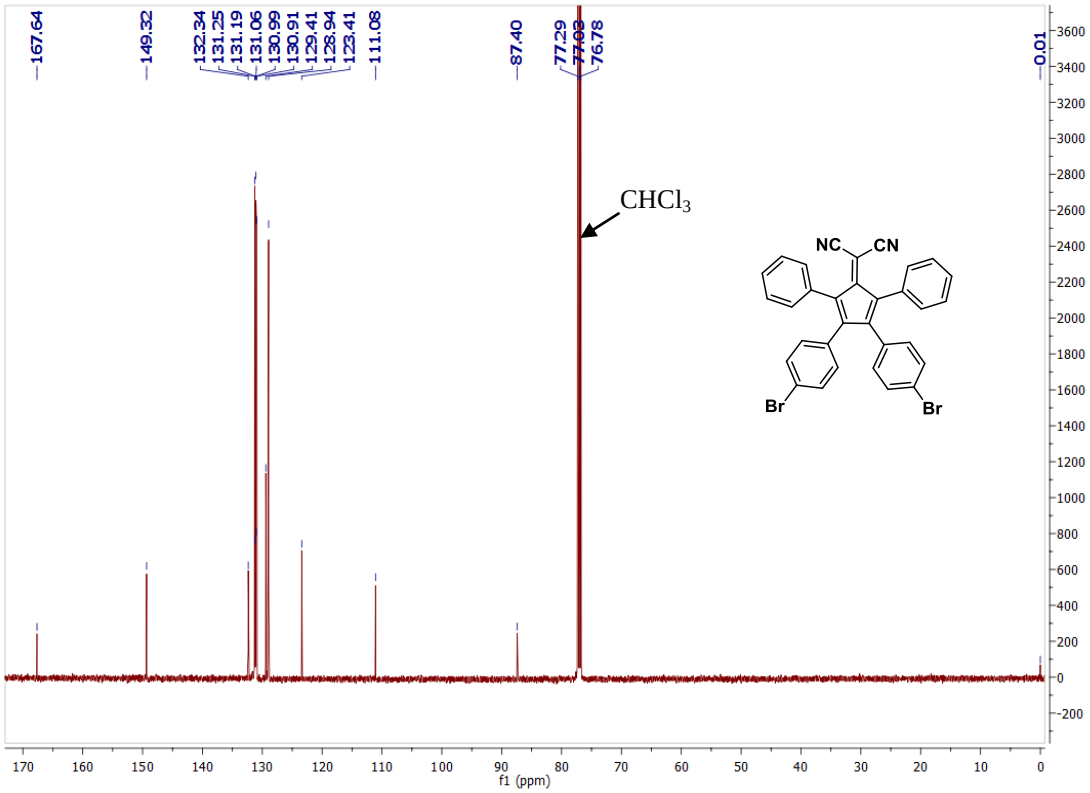

Fig. S33A: ESI-MS spectrum of compound 2a:

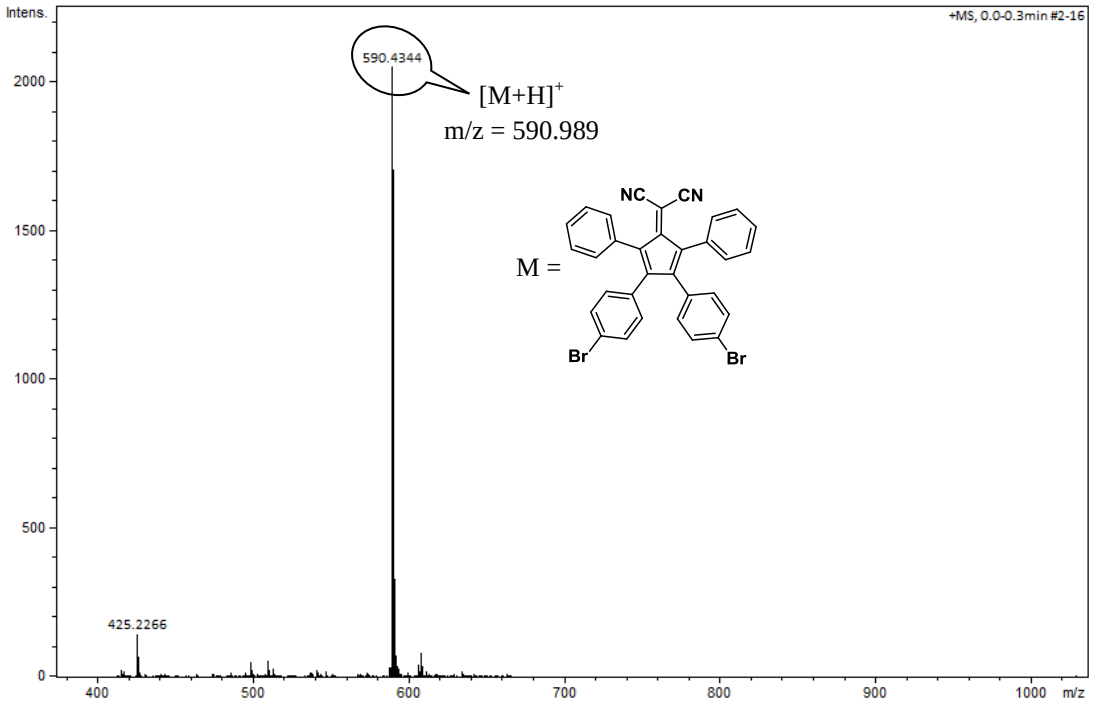

Fig. S33B: FT-IR spectrum of 2a:

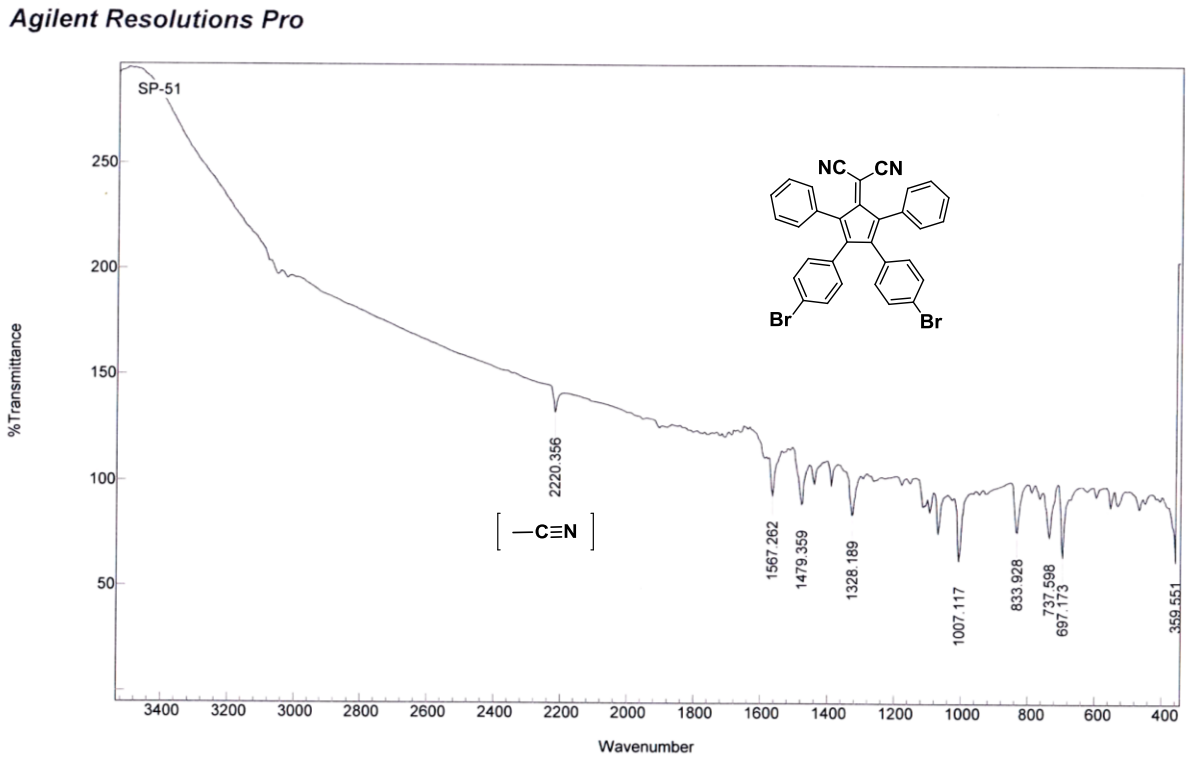

Fig. S34A: ^{1}H NMR Spectra ($CDCl_3$, 500 MHz, ppm) of compound 2b:

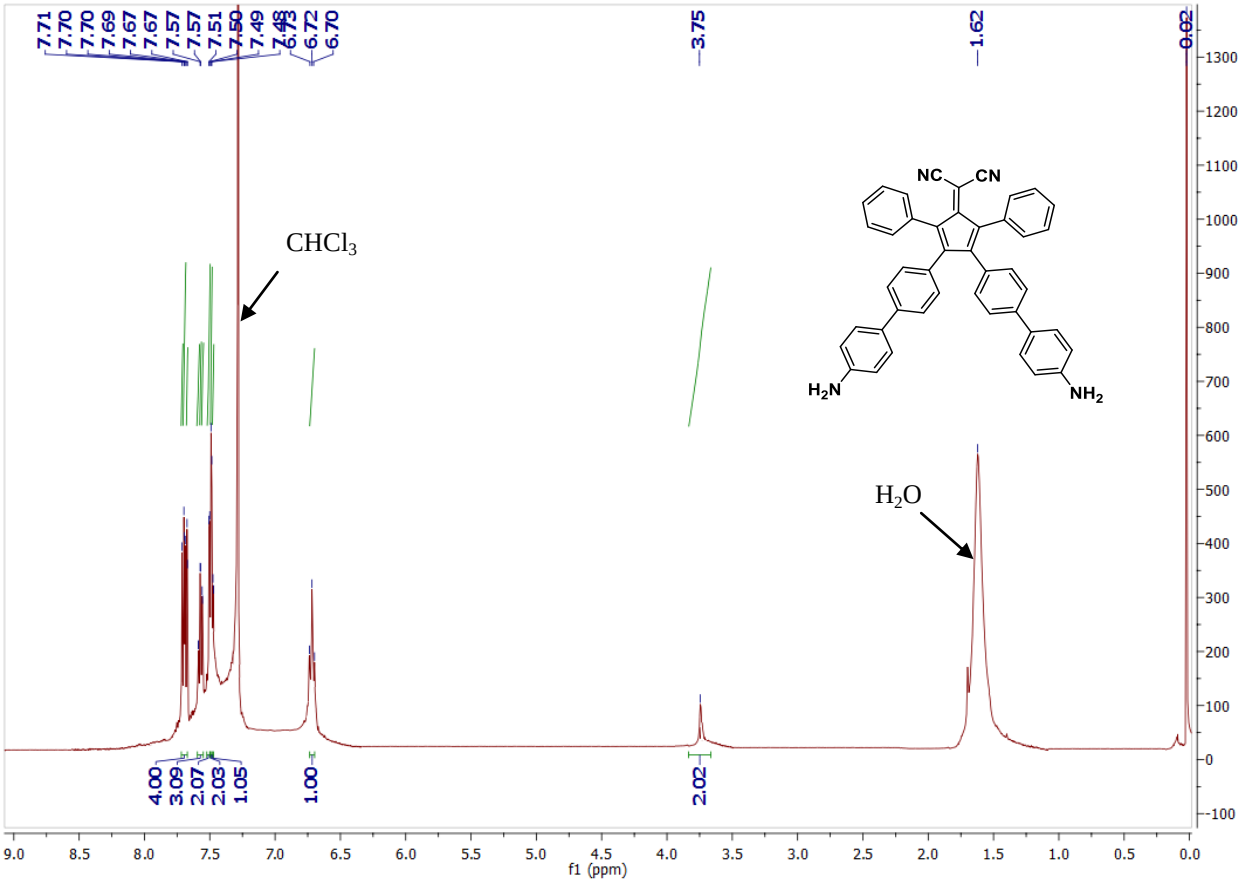

Fig. S34B: ^{13}C Spectra ($CDCl_3$, 125 MHz, ppm) of compound 2b:

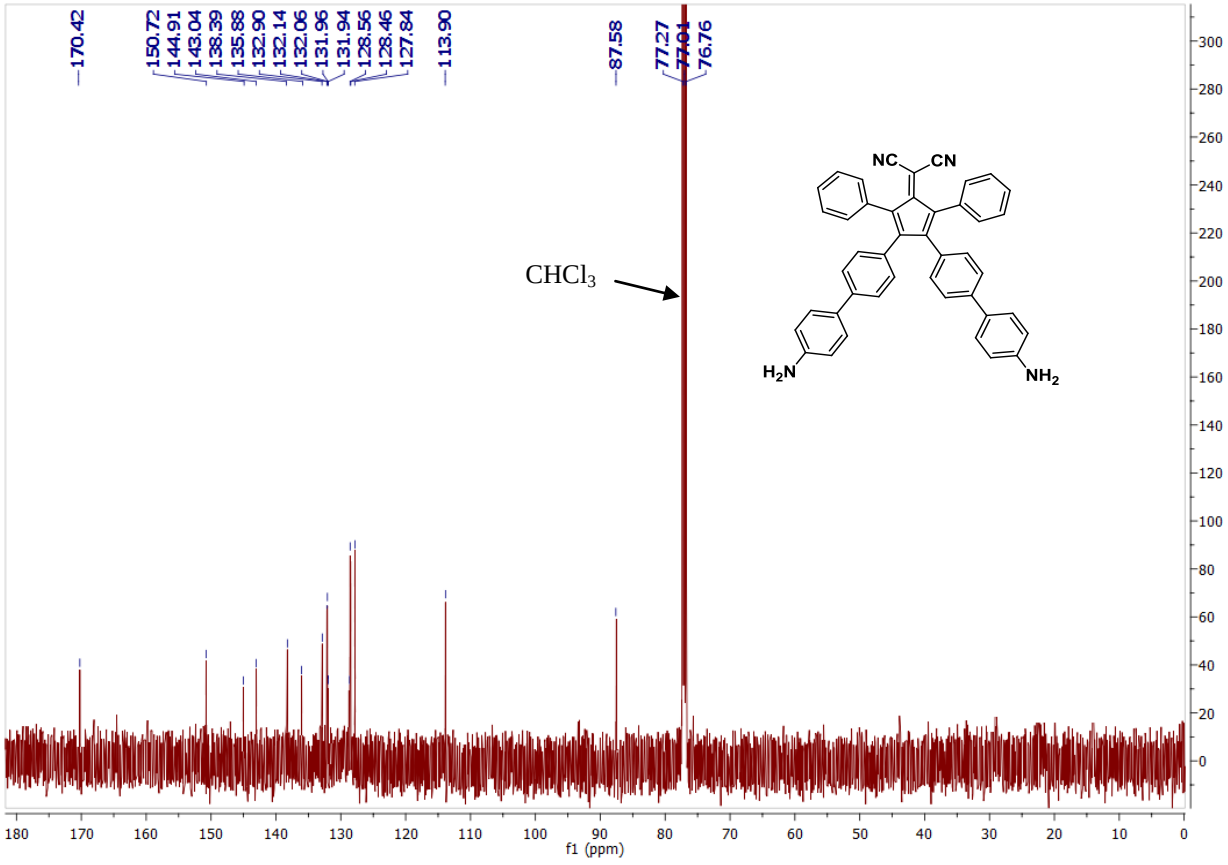

Fig. S35A: ESI-MS spectrum of compound 2b:

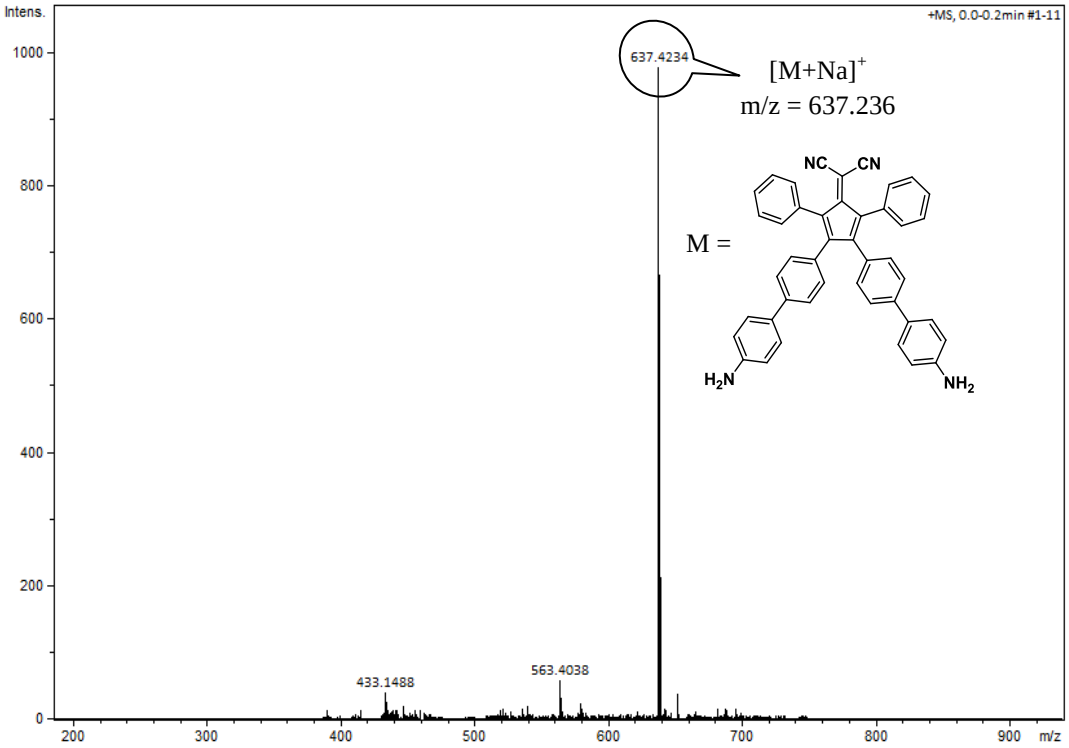

Fig. S35B: FT-IR spectrum of 2b:

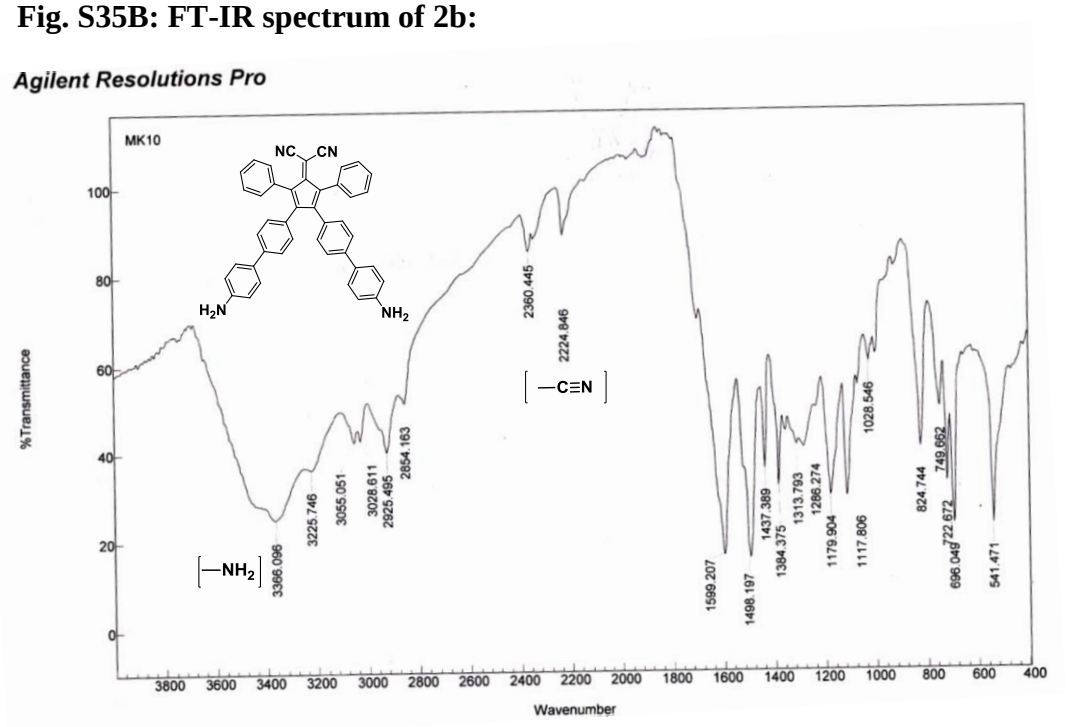

Fig. S36A: ^{1}H NMR Spectra (DMSO-d_6, 500 MHz, ppm) of compound 4:

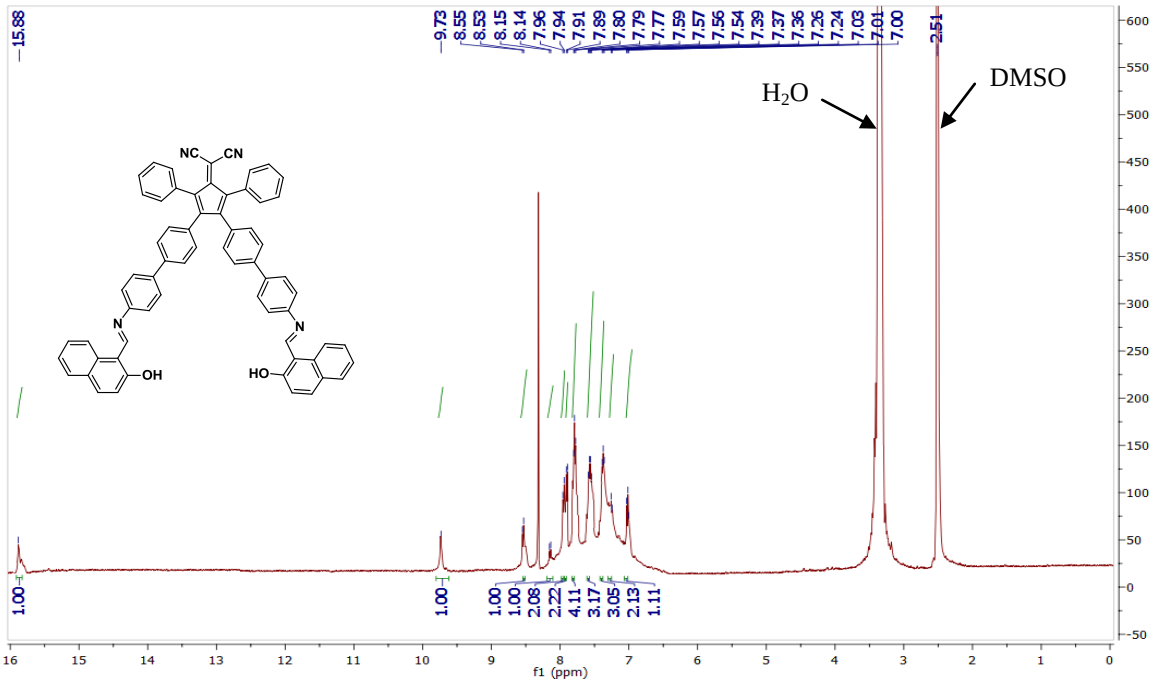

Fig. S36B: ^{13}C Spectra ($CDCl_3$, 125 MHz, ppm) of compound 4:

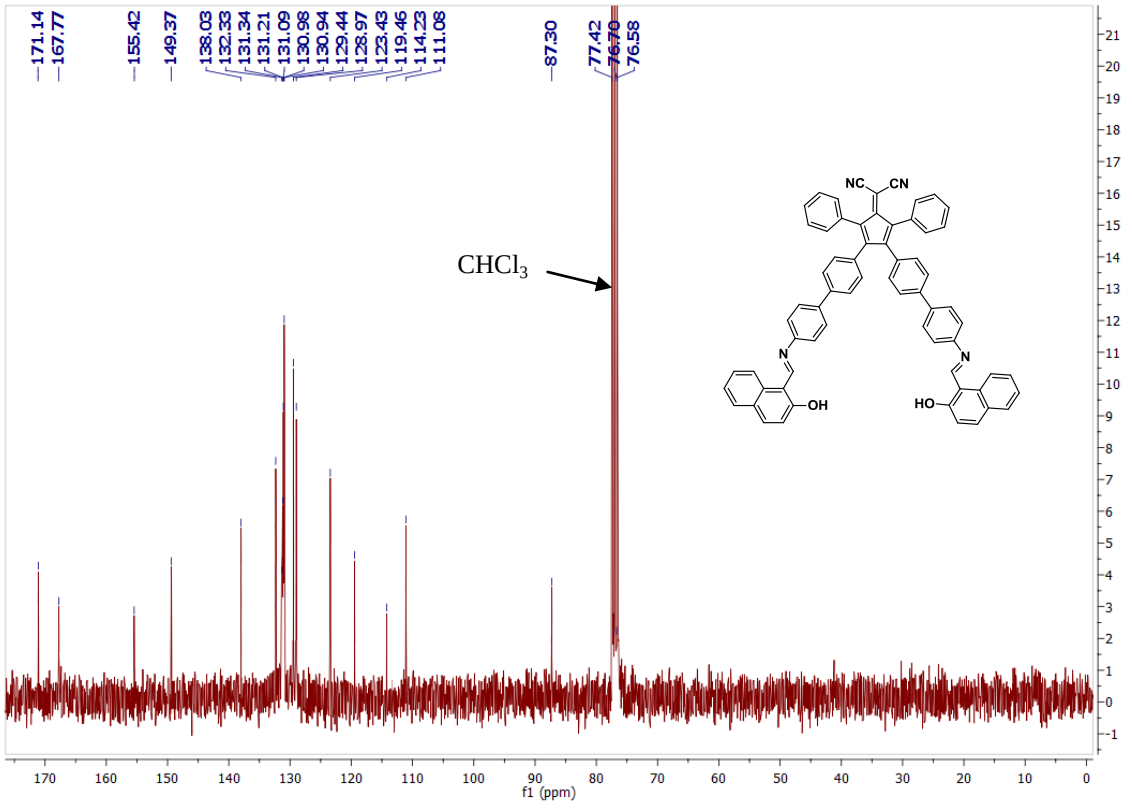

Fig. S37A: ESI-MS spectrum of compound 4:

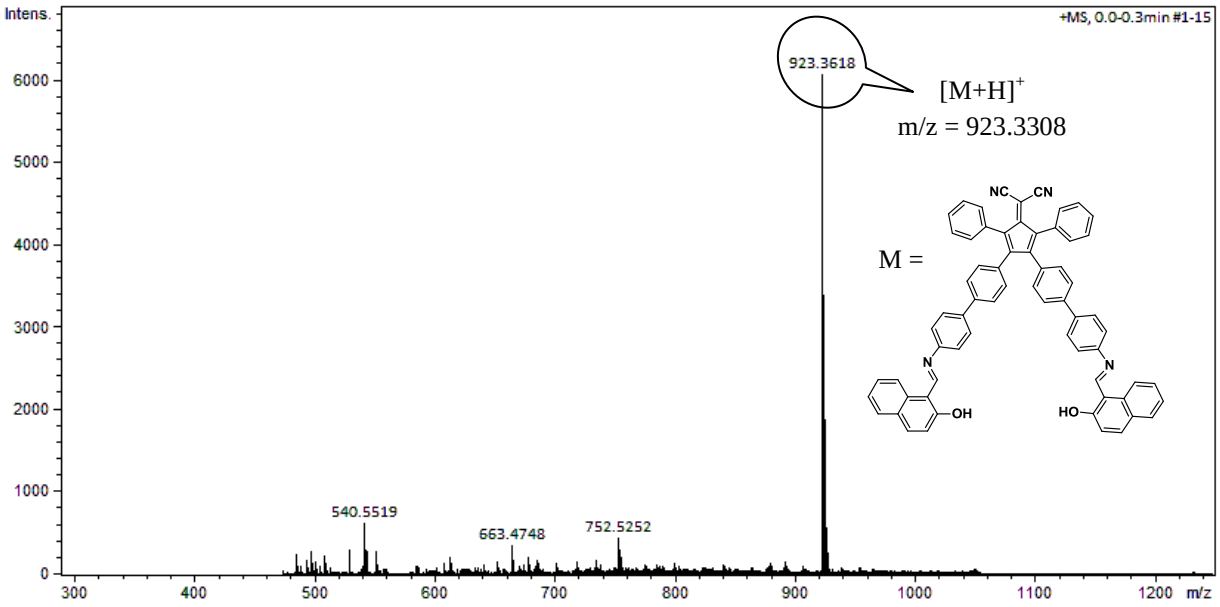

Fig. S37B: FT-IR Spectrum of compound 4: